# Temperatures from Energy Balance Models: the effective heat capacity matters

Gerrit Lohmann[1,2]

[1]Alfred Wegener Institute, Helmholtz Centre for Polar and Marine Research, Bremerhaven, Germany
[2] University of Bremen, Bremen, Germany

**Correspondence:** Gerrit Lohmann (Gerrit.Lohmann@awi.de)

**Abstract.** Energy balance models (EBM) are highly simplified systems of the climate system. The global temperature is calculated by the radiation budget through the incoming energy from the Sun and the outgoing energy from the Earth. The argument that the temperature can be calculated by the simple radiation budget is revisited. The underlying assumption for a realistic temperature distribution is explored: One has to assume a moderate diurnal cycle due to the large heat capacity and the fast rotation of the Earth. Interestingly, the global mean in the revised EBM is very close to the originally proposed value. A linearized EBM implicitly assumes the heat capacity and the fast rotation arguments. The main point is, that the effective heat capacity and its temporal variation over the daily/seasonal cycle needs to be taken into account when estimating surface temperature from the energy budget. The time dependent-EBM predicts a flat meridional temperature gradient for large heat capacities~~which can be related to very effective vertical diffusion.~~ . Motivated by this finding, ~~sensitivity experiments~~ a sensitivity experiment with a complex model ~~are~~ is performed where the vertical diffusion in the ocean has been increased. The resulting ~~climate shows a~~ flat meridional temperature gradient and ~~a deeper thermocline.~~ reduced seasonal cycle is also found in climate reconstructions, ~~The common pattern of surface temperature anomalies and climate reconstructions suggests~~ suggesting a possible mechanism for past climate changes prior to 3 million years ago.

**Keywords.** Energy balance model, Earth system modeling, Temperature gradient, Climate change, Climate sensitivity, Climate reconstructions

## 1 Introduction

Energy balance models (EBMs) are among the simplest climate models. They were introduced almost simultaneously by Budyko (1969) and Sellers (1969). Because of their simplicity, these models are easy to understand and facilitate both analytical and numerical studies of climate sensitivity (Peixoto and Oort, 1992; Hartmann, 1994; Saltzmann, 2001; Ruddiman, 2001; Pierrehumbert, 2010). A key feature of these models is that they eliminate the climate's dependence on the wind field, ocean currents, the Earth rotation, and thus have only one dependent variable: the Earth's near-surface air temperature T.

With the development of computer capacities, simpler models have not disappeared; on the contrary, a stronger emphasis has been given to the concept of a hierarchy of models' as the only way to provide a linkage between theoretical understanding and the complexity of realistic models (von Storch et al. 1999; Claussen et al. 2002). In contrast, many important scientific

debates in recent years have had their origin in the use of conceptually simple models (Le Treut et al., 2007; Stocker, 2011), also as a way to analyze data (Köhler et al., 2010) or complex models (Knorr et al., 2011).

Pioneering work has been done by North (North, 1975a, b; 1981; 1983) and these models were applied subsequently (e.g., Ghil, 1976; Su and Hsieh, 1976; Ghil and Childress, 1987; Short et al., 1991; Stocker et al., 1992; North and Kim, 2017). Later the EMBs were equipped by the hydrological cycle (Chen et al., 1995; Lohmann et al., 1996; Fanning and Weaver ,1996; Lohmann and Gerdes, 1998) to study the feedbacks in the atmosphere-ocean-sea ice system. One of the most useful examples of a simple, but powerful, model is the one-/zero-dimensional energy balance model. As a starting point, a zero-dimensional model of the radiative equilibrium of the Earth is introduced (Fig. 1)

$$(1-\alpha)S\pi R^2 = 4\pi R^2 \epsilon \sigma T^4 \tag{1}$$

where the left hand side represents the incoming energy from the Sun (size of the disk= shadow area $\pi R^2$) while the right hand side represents the outgoing energy from the Earth (Fig. 1). T is calculated from the Stefan-Boltzmann law assuming a constant radiative temperature, S is the solar constant - the incoming solar radiation per unit area– about ~~$1367 W m^{-2}$~~ $1367\,\mathrm{Wm^{-2}}$, $\alpha$ is the Earth's average planetary albedo, measured to be 0.3. R is Earth's radius = ~~$6.371 \times 10^6$~~ $6.371 \cdot 10^6$ m, $\sigma$ is the Stefan-Boltzmann constant = ~~$5.67 \times 10^{-8} \mathrm{JK^{-4}m^{-2}s^{-1}}$~~ $5.67 \cdot 10^{-8} \mathrm{JK^{-4}m^{-2}s^{-1}}$, and $\epsilon$ is the effective emissivity of Earth (about 0.612) (e.g., Archer 2010). The geometrical constant $\pi R^2$ can be factored out, giving

$$(1-\alpha)S = 4\epsilon\sigma T^4 \tag{2}$$

Solving for the temperature,

$$T = \sqrt[4]{\frac{(1-\alpha)S}{4\epsilon\sigma}} \tag{3}$$

Since the use of the effective emissivity $\epsilon$ in (1) already accounts for the greenhouse effect we gain an average Earth temperature of 288 K (15°C), very close to the global temperature observations/reconstructions (Hansen et al., 2011) at 14°C for 1951-1980. Interestingly, (3) does not contain parameters like the heat capacity of the planet. We will explore that this is essential for the temperature of the Earth's climate system.

Schwartz (2007) stressed out that the effective heat capacity is not an intrinsic property of the climate system but is reflective of the rate of penetration of heat energy into the ocean in response to the particular pattern of forcing and background state. We will evaluate the effect of the effective heat capacity in the climate system. Wang et al. (2019) showed a pronounced low equator-to-pole gradient in the annual mean sea surface temperatures is found in a numerical experiment conducted with a coupled model consisting of an atmospheric general circulation model coupled to a slab ocean model in which the mixed-layer thickness is reduced. In the present paper, it is shown that the heat capacity is linked to the long-lasting question of a low equator-to-pole gradients during the Paleogene/Neogene climate (Markwick, 1994; Wolfe, 1994; Sloan and Rea, 1996; Huber et al., 2000; Shellito et al., 2003; Tripati et al., 2003; Mosbrugger et al., 2005). Those published temperature patterns resemble the high latitude warming (with moderate low latitude warming) and reduced seasonality.

## 2 A closer look onto the spatial distribution

Let us have a closer look onto (1) ~~. The~~ and consider local radiative equilibrium of the Earth ~~is~~ at each point. Fig. 2 shows the latittude-longitude dependence of the incoming short wave radiation. The global mean temperatures are not affected by the tilt (Berger and Loutre 1991; 1997; Laepple and Lohmann 2009). We assume an idealized geometry of the Earth, no obliquity and no precession, which makes an analytical calculation possible.

The incoming radiation goes with the cosine of latitude $\varphi$ and longitude $\Theta$, and there is only sunshine during the day. Fig. 2a shows the latitudinal dependence. As we assume no tilt (this assumption is later relaxed), the latitudinal dependence is a function of latitude only: $\cos\varphi$. On the right-hand side, the function is shown. Fig. 2b shows the latitudinal dependence is a function of longitude: $\cos\Theta$ for the sun-shining side of the Earth, and for the dark side of the Earth it is zero. For simplicity, we can define the angle $\Theta$ anti-clockwise on the for the sun-shining side between $-\pi/2$ and $\pi/2$. We define the maximal insolation always at $\Theta = 0$ which is moving in time. In the panel, the Earth's rotation is schematically sketched as the red arrow, and we see the time-dependence in the right-hand side. It is noted that the geographical longitude can be calculated by $mod(\Theta - 2\pi \cdot t/24, 2\pi)$ where t is measured in hours and mod is the modulo operation. Summarizing our geometrical considerations, we can now write the local energy balance as

$$\epsilon\sigma T^4 = (1-\alpha)S\cos\varphi\cos\Theta\times 1_{[-\pi/2<\Theta<\pi/2]}(\Theta)\cdot\cos\varphi\cdot\cos\Theta \qquad \text{for } -\pi/2<\Theta<\pi/2 \tag{4}$$

~~where $\varphi$ and $\Theta$ are the latitude and longitute, respectively. Integration~~ and zero during night for $\Theta < -\pi/2$ or $\Theta > \pi/2$. Temperatures based on the local energy balance without a heat capacity would vary between $T_{min} = 0$ K and $T_{max} = \sqrt[4]{\frac{(1-\alpha)S}{\epsilon\sigma}} = \sqrt{2}\cdot\sqrt[4]{($ K.

Integration of (4) over the Earth surface is

$$\begin{aligned}
\int_{-\pi/2}^{\pi/2}\left(\int_0^{2\pi}\epsilon\sigma T^4 R\cos\varphi d\Theta\right)Rd\varphi &= (1-\alpha)S\int_{-\pi/2}^{\pi/2}R\cos^2\varphi d\varphi\cdot\int_{-\pi/2}^{\pi/2}R\cos\Theta d\Theta \\
\epsilon\sigma R^2\frac{4\pi}{4\pi}\int_{-\pi/2}^{\pi/2}\left(\int_0^{2\pi}T^4\cos\varphi d\Theta\right)d\varphi &= (1-\alpha)SR^2\underbrace{\int_{-\pi/2}^{\pi/2}\cos^2\varphi\, d\varphi}_{\frac{\pi}{2}}\cdot\underbrace{\int_{-\pi/2}^{\pi/2}\cos\Theta\, d\Theta}_{2} \\
\epsilon\sigma 4\pi\overline{T^4} &= (1-\alpha)S\,\pi
\end{aligned} \tag{5}$$

giving a similar formula as (3) with the definition for the average $\overline{T^4}$.

What we really want is the mean of the temperature $\overline{T}$. Therefore, we take the fourth root of (4):

$$T = \sqrt[4]{\frac{(1-\alpha)S\cos\varphi\cos\Theta}{\epsilon\sigma}}\times 1_{[-\pi/2<\Theta<\pi/2]}(\Theta). \qquad \text{for } -\pi/2<\Theta<\pi/2 \tag{6}$$

and zero elsewhere. If we calculate the zonal mean of (6) by integration at the latitudinal cycles we have

$$T(\varphi) = \frac{1}{2\pi}\int_{-\pi/2}^{-\pi/2}\sqrt[4]{\frac{(1-\alpha)S\cos\varphi\cos\Theta}{\epsilon\sigma}}d\Theta$$

$$= \frac{\sqrt{2}}{2\pi}\underbrace{\int_{-\pi/2}^{\pi/2}(\cos\Theta)^{1/4}d\Theta}_{2.700\sqrt{\pi}\Gamma(5/8)/\Gamma(9/8)}\sqrt[4]{\frac{(1-\alpha)S}{4\epsilon\sigma}}(\cos\varphi)^{1/4} = 0.608\underbrace{\frac{1}{\sqrt{2\pi}}\frac{\Gamma(5/8)}{\Gamma(9/8)}}_{\approx 0.608}\cdot\sqrt[4]{\frac{(1-\alpha)S}{4\epsilon\sigma}}(\cos\varphi)^{1/4} \quad (7)$$

as a function on latitude (Fig. 3). $\Gamma$ is Euler's Gamma function with $\Gamma(x+1) = x\Gamma(x)$. When we integrate this over the latitudes, we obtain

$$\overline{T} = \frac{1}{2}\int_{-\pi/2}^{\pi/2}T(\varphi)\cos\varphi d\varphi = \frac{0.608}{2}\frac{1}{2}\frac{\Gamma(5/8)}{\sqrt{2\pi}\Gamma(9/8)}\cdot\sqrt[4]{\frac{(1-\alpha)S}{4\epsilon\sigma}}\underbrace{\int_{-\pi/2}^{\pi/2}(\cos\varphi)^{5/4}d\varphi}_{1.862\sqrt{\pi}\Gamma(9/8)/\Gamma(13/8)}$$

$$= \underbrace{0.4\sqrt{2}}_{\approx}\frac{1}{2}\frac{1}{\sqrt{2}}\frac{\Gamma(5/8)}{\Gamma(13/8)}\cdot\sqrt[4]{\frac{(1-\alpha)S}{4\epsilon\sigma}} = 0.566\underbrace{\frac{\sqrt{2}}{4}\frac{8}{5}}_{0.4\sqrt{2}\approx 0.566}\cdot\sqrt[4]{\frac{(1-\alpha)S}{4\epsilon\sigma}} \quad (8)$$

Therefore, ~~$\overline{T} = 163$K~~ the mean temperature is a factor ~~0.566~~ $0.4\sqrt{2} \approx 0.566$ lower than 288 K as stated at ~~(1)~~ 3) and would be $\overline{T} = 163$ K. The standard EBM in Fig. 1 has imprinted into our thoughts and lectures. We should therefore be careful and pinpoint the reasons for the failure.

What happens here is that the heat capacity of the Earth is neglected ~~. During night, the temperature is very low~~ and there is a strong non-linearity of the outgoing radiation. ~~Furthermore, the Earth is a rapidly rotating object. Equation (6) can be better used for objects like the Moon or Mercury (Vasavada et al., 1999) as slowly rotating bodies without significant heat capacity.~~

## 3 The heat capacity and fast rotating body

The energy balance shall take the heat capacity into account:

$$C_p\partial_t T = (\underbrace{1-1}_{=}-\alpha)S\underbrace{\cos\varphi\cos\Theta\cdot\cos\varphi\cdot\cos\Theta}_{-\epsilon\sigma T^4}\underbrace{\times 1_{[-\pi/2<\Theta<\pi/2]}(\Theta)}_{\text{elsewhere}} \quad \text{for } -\pi/2 < \Theta < \pi/2$$

$$= -\epsilon\sigma T^4 \quad (9)$$

with $C_p$ representing the heat capacity multiplied with the depth of the atmosphere-ocean layer ($C_p$ is in the order of $10^7 - 10^8 JK^{-1}m^{-2}$). If we consider the zonal mean and averaged over the diurnal cycle, we can assume that the heat capacity is mainly given by the ~~ocean~~atmosphere and the uppermost ocean and soil. Observational evidence is that the diurnal variation of the ocean surface is in the order of 0.5-3 K with highest values at favorable conditions of high insolation and low winds (Stommel, 1969; Anderson et al., 1996; Kawai and Kawamura, 2002; Stuart-Menteth, et al. 2003; Ward, 2006). ~~A significant~~

~~heat capacity damping the surface temperatures are furthermore found over ice and soil. The atmospheric circulation provides an efficient way to propagate heat along latitudes which is ignored and is a second order effect (not shown). The energy balance (9)~~ To simplify (9), the energy balance is integrated over the longitude and ~~over the day~~day, and assume that the variation due to the diurnal cycle is weak. With $\tilde{T} = \frac{1}{2\pi}\int_0^{2\pi} T\, d\Theta$, we find

$$\tilde{T}(\tilde{t}) = \frac{1}{2\pi}\int_0^{2\pi} T(t)\, d\Theta \quad \text{with} \quad \tilde{T}^4 \approx \frac{1}{2\pi}\int_0^{2\pi} T^4\, d\Theta$$

~~and therefore~~

$$C_p \partial_t \tilde{T} = (1-\alpha) S \cos\varphi \cdot \underbrace{\frac{1}{2\pi}\int_{-\pi/2}^{\pi/2} \cos\Theta\, d\Theta}_{2} - \epsilon\sigma \tilde{T}^4 \underbrace{\frac{1}{2\pi}\int_0^{2\pi} T^4\, d\Theta}_{\approx \tilde{T}^4} = (1-\alpha)\frac{S}{\pi}\cos\varphi - \epsilon\sigma\tilde{T}^4 \tag{10}$$

giving the equilibrium solution

$$\tilde{T}(\varphi) = \sqrt[4]{\frac{4}{\pi}} \cdot \sqrt[4]{\frac{(1-\alpha)S}{4\epsilon\sigma}} \quad (\cos\varphi)^{1/4} \tag{11}$$

shown in Fig. 3 as the read line~~with the mean~~. The global mean temperature is

$$\overline{\tilde{T}} = \sqrt[4]{\frac{4}{\pi}} \cdot \sqrt[4]{\frac{(1-\alpha)S}{4\epsilon\sigma}} \quad \underbrace{\frac{1}{2}\int_{-\pi/2}^{\pi/2} (\cos\varphi)^{5/4} d\varphi}_{1.862/\sqrt{\pi}\,\Gamma(9/8)/\Gamma(13/8)} = \sqrt[4]{\frac{4}{\pi}}\frac{1.862}{2} \quad \underbrace{\sqrt{\frac{\pi}{2}}\frac{\Gamma(9/8)}{\Gamma(13/8)}}_{\approx 0.989} \cdot \sqrt[4]{\frac{(1-\alpha)S}{4\epsilon\sigma}} = 0.989 \sqrt[4]{\frac{(1-\alpha)S}{4\epsilon\sigma}} \approx 28$$

~~Therefore, $\overline{\tilde{T}} = 285 \approx 288$ K, very similar as in (1).~~ which is very similar to 288 K from (3).

A numerical solution of (9) is shown as the brownish dashed line in Fig. 3 where the diurnal cycle has been taken into account and $C_p = C_p^a$ has been chosen as the atmospheric heat capacity

$$C_p^a = c_p p_s/g = 1004\, JK^{-1}kg^{-1} \cdot 10^5 Pa/(9.81 ms^{-2}) = 1.02 \cdot 10^7 JK^{-1}m^{-2}$$

which is the specific heat at constant pressure $c_p$ times the total mass $p_s/g$. $p_s$ is the surface pressure and $g$ the gravity. The global mean temperature $\overline{T}$ is 286 K, again close to 288 K.

Quite often the linearization the long wave radiation $\epsilon\sigma T^4$ is linearized in energy balance models. Indeed the linearization is performed around $0°C$ (North et al., 1975a, b; Chen et al., 1995; Lohmann and Gerdes, 1998; North and Kim, 2017) and is formulated as $A + B \cdot T'$ with $T'$ being measured in $°C$. As the temperatures based on the local energy balance without a heat capacity would vary between $T_{min} = 0$ K and $T_{max} = \sqrt{2} \cdot 288K = 407$ K, a linearization would be not permitted. Therefore, the linearization implicitely assumes the above heat capacity and fast rotation arguments.

The effect of heat capacity is systematically analyzed in Fig. 4. The temperatures are relative insensitive for a wide range of $C_p$. We find a severe drop in temperatures for heat capacities below $0.01$ of the atmospheric heat capacity $C_p^a$. ~~We find~~

~~furthermore~~ Fig. 5 shows the temperature dependence for different values of $C_p$ and the length of the day, indicating a pronounced temperature drop during night for low values of heat capacities and for ~~long days (e.g.~~ (hypothetical) long days of 240 h instead of 24 h~~) affecting the zonal temperatures (4.5 K colder at the equator). It is an interesting thought experiment what would happen if the length of the daylight/night would change.~~ . We have chosen this feature for a particular latitude (here: $45^0$N). The analysis shows that the effective heat capacity is of great importance for the temperature, this depends on the atmospheric planetary boundary layer (how well-mixed with small gradients in the vertical) and the depth of the mixed layer in the ocean ~~. To make a rough estimate of the involved mixed layer, one can see that the effective heat capacity of the ocean is time-scale dependent. A diffusive heat flux goes down the gradient of temperature and the convergence of this heat flux drives a ocean temperature tendency:~~

~~where $k_v = k^o/C_p^o$ is the oceanic vertical eddy diffusivity in $m^2\,s^{-1}$, and $C_p^o$ the oceanic heat capacity relevant on the specific time scale. The vertical eddy diffusivity $k_v$ can be estimated from climatological hydrographic data (Olbers et al., 1985; Munk and Wunsch, 1998) and varies roughly between $10^{-5}$ and $10^{-4}\,m^2\,s^{-1}$ depending on depth and region. A scale analysis of (15) yields a characteristic depth scale $h_T$ through For the diurnal cycle $h_T$ is less that half a meter and the heat capacity generally less than that of the atmosphere. As pointed out by Schwartz (2007), the effective heat capacity that reflects only that portion of the global heat capacity that is coupled to the perturbation on the timescale of the perturbation. We discuss the sensitivity of the system with respect to $k_v$ laterin the context of a full circulation model~~which will be analyzed later.

## 4 Meridional temperature gradients

Equation (10) shall be the starting point for further investigations. One can easily include the ~~meriodional~~ meridional heat transport by diffusion which has been previously used in one-dimensional EBMs (e.g. Adem, 1965; Sellers, 1969; Budyko, 1969; North, 1975a,b). In the following we will drop the tilde sign. Using a diffusion coefficient k, the meridional heat transport across a latitude is $HT = -k\nabla T$. One can solve the EBM

$$C_p\,\partial_t T = \nabla \cdot HT + (1-\alpha)\frac{S}{\pi}\cos\varphi - \epsilon\sigma T^4 \quad . \tag{13}$$

numerically. The boundary condition is that the HT at the poles vanish. The values of k are in the range of earlier studies (North, 1975a,b; Stocker et al., 1992; Chen et al., 1995; Lohmann et al., 1996). Fig. 6 shows the equilibrium solutions of (13) using different values of $k$ (solid lines). The global mean temperature is not affected by the transport term because of the boundary condition with zero heat transport at the poles. The same is true if we introduce zonal transports because of the cyclic boundary condition in $\theta-$direction.

Until now, we assumed that the Earth's axis of rotation were vertical with respect to the path of its orbit around the Sun. Instead Earth's axis is tilted off vertical by about 23.5 degrees. As the Earth orbits the Sun, the tilt causes one hemisphere to receive more direct sunlight and to have longer days. This is a redistribution of heat with more solar insolation at the poles and less at the equator (formally it could be associated to an enhanced meridional heat transport HT). The resulting temperature is shown as the dotted blue line in Fig. 6. A spatially constant temperature in (1) can be formally seen as a system with infinite diffusion coefficient $k \to \infty$ (black line in Fig. 6).

The global mean temperatures are not affected by the tilt and the values are identical to the one calculated in (12). This is true even if we calculate the seasonal cycle (Berger and Loutre, 1991; 1997; Laepple and Lohmann, 2009). However, if we include non-linearities such as the ice-albedo feedback ($\alpha$ as a function of T), the global mean value is changing (Budyko, 1969; Sellers, 1969; North et al., 1975a, b), cf. the dashed blue line in Fig. 6. Such model can be improved by including an explicit spatial pattern with a seasonal cycle to study the long-term effects of climate to external forcing (Adem, 1981; North et al., 1983) or by adding noise mimicking the effect of short-term features on the long-term climate (Hasselmann, 1976; Lemke, 1977; Lohmann, 2018).

As a logical next step, let us now include an explicit seasonal cycle into the EBM:

$$C_p \partial_t T = \nabla \cdot HT + (1-\alpha)S(\varphi,t) - \epsilon\sigma T^4 \quad . \tag{14}$$

with $S(\varphi,t)$ being calculated daily (Berger and Loutre, 1991; 1997). Eq. (14) is calculated numerically for fixed diffusion coefficient $k = 1.5 \cdot 10^6 m^2/s$ under present orbital conditions. Fig. 7 indicates that the temperature gradient is getting flatter for large heat capacities. Furthermore, the mean temperature is affected by the choice of $C_p$. In the case of large heat capacity at high latitudes (for latitudes polewards of $\varphi = 50°$) and moderate elsewhere, we observe strong warming at high latitudes with moderate warming at low latitudes (dashed curve). This again indicates that we cannot neglect the time-dependent left hand side in the energy balance equations, both for the diurnal (9) as well as the seasonal (14) cycle for the temperature budget. In both considered cases, at strong diurnal ~~/~~or seasonal amplitude lowers the annual mean temperature.

Fig. 8 shows the seasonal amplitude for the $C_p$-scenarios as indicated by the blue and dashed black lines, respectively. ~~A change in the seasonal /diurnal cycle of $T_1 - T_2 = 50°$C is equivalent to about $10 Wm^{-2}$ when applying the long wave radiation change $\epsilon\sigma \cdot 0.5(T_1^4 + T_2^4) - \epsilon\sigma \cdot (0.5 \cdot (T_1 + T_2))^4$ for typical temperatures on the Earth. Please note that the number $10 Wm^{-2}$ is equivalent to a greenhouse gas forcing of more than quadrupling the $CO_2$ concentration in the atmosphere.~~

## 5 ~~Meridional temperature gradient in a complex model~~

~~Energy balance models have been used to diagose the temperatures on the Earth when applying complex circulation models (e.g., Knorr et al. 2011)or data (e.g., Köhler et al., 2010; van der Heydt et al., 2016; Stap~~ The larger the seasonal contrast, the colder is the climate. Let us define here $\bar{\cdot}$ as the averaging over a time period (here the seasonal cycle), then $\overline{T^4} > \overline{T}^4$ which is consistent with Hölder's inequality (Rodgers, 1888; Hölder 1889; Hardy et al., ~~2018). For the past, a strong warming at high latitudes is reconstructed for the Pliocene, Miocene, Eocene periods (Markwick, 1994; Wolfe, 1994; Sloan and Rea, 1996; Huber et al. , 2000; Shellito et al. , 2003; Tripati et al. , 2003; Mosbrugger et al., 2005; Utescher and Mosbrugger, 2007).~~ 1934, Kuptsov, 2001). It is noted that this feature is missing in the linearized version $A + B \cdot T'$ of the outgoing radiation. We see the large variation in the seasonal cycle $\Delta T = T_{summer} - T_{winter}$ for the blue line in Fig. 8 as compared to the dashed line. A mean change in the net long wave radiation can be approximated by the mean of summer and winter values $\epsilon\sigma \cdot 0.5(T_{summer}^4 + T_{winter}^4)$, which is up to $10 Wm^{-2}$ higher than $\epsilon\sigma \cdot (0.5 \cdot (T_{summer} + T_{winter}))^4$ if the seasonal cycle is damped as in the dashed line of Fig. 8. This implies that a lower seasonal cycle provides for a significant warming. If we would

consider a linear model $A + B \cdot T'$ with $T'$ being measured in $°C$ for the long-wave radiation, the differences between the blue and the dashed line would be much lower, due to the absence of the non-linearity in net long wave radiation change.

## 5 Meridional temperature gradient in a complex model

In the following~~this period is called Paleogene/Neogene, which covers the period $3 \cdot 10^6 - 65 \cdot 10^6$ years ago. Until now, it is a conundrum that the modelled high latitudes are not as warm as the reconstructions (e. g., Sloan and Rea, 1996; Huber et al. , 2000; Mosbrugger~~ a complex circulation model is used where the seasonal cycle is reduced by enhanced vertical mixing in the ocean. To make a rough estimate of the involved mixed layer, one can see that the effective heat capacity of the ocean is time-scale dependent. A diffusive heat flux goes down the gradient of temperature and the convergence of this heat flux drives a ocean temperature tendency:

$$C_p^o \partial_t T = -\partial_z (k^o \partial_z T) \tag{15}$$

where $k_v = k^o / C_p^o$ is the oceanic vertical eddy diffusivity in $m^2\, s^{-1}$, and $C_p^o$ the oceanic heat capacity relevant on the specific time scale. The vertical eddy diffusivity $k_v$ can be estimated from climatological hydrographic data (Olbers et al., ~~2005; Knorr et al., 2011; Dowset et al., 2013) . Inspired by Fig. 7, we may think of a climate system having a higher net heat capacity $C_p$ producing flat temperature gradients. Another argument comes from data.La Riviere~~ 1985; Munk and Wunsch, 1998) and varies roughly between $10^{-5}$ and $10^{-4}\, m^2\, s^{-1}$ depending on depth and region. A scale analysis of (15) yields a characteristic depth scale $h_T$ through

$$\frac{\Delta T}{\Delta t} = k_v \frac{\Delta T}{h_T^2} \quad \longrightarrow h_T = \sqrt{k_v\, \Delta t} \tag{16}$$

For the diurnal cycle $h_T$ is less that half a meter and the heat capacity generally less than that of the atmosphere. The seasonal mixed layer depth can be several hundred meters (e.g., de Boyer Montégut et al.~~(2012)showed that the oceanic state in the Paleogene/Neogene had a deeper thermocline, high sea surface temperatures, and low temperature gradients. Global climate models treat ocean vertical mixing as static, although there is little reason to suspect this is correct (e. g., see Munk and Wunsch, 1998). ~~, 2004). As pointed out by Schwartz (2007), the effective heat capacity that reflects only that portion of the global heat capacity that is coupled to the perturbation on the timescale of the perturbation. In the context of global climate change induced by changes in atmospheric composition on the decade to century timescale the effective heat capacity is subject to change in heat content on such timescales.

In order to test the effective heat capacity/mixing hypothesis, we employ the coupled climate model COSMOS which was developed at the Max-Planck Institute for Meteorology in Hamburg (Jungclaus et al., 2000). The model contains explicit diurnal and seasonal cycles, it has no flux correction and has been successfully applied to test a variety of paleoclimate hypotheses, ranging from the Miocene climate (Knorr et al., 2011; Knorr and Lohmann, 2014; Stein et al., 2016), the Pliocene (Stepanek and Lohmann, 2012) as well as glacial (Zhang et al., 2013; 2014) and interglacial climates (Wei and Lohmann, 2012; Lohmann et al., 2013; Pfeiffer and Lohmann, 2016).

~~Paleogene/Neogene simulations which were published so far show the underestimated flat temperature gradients as compared to data. As pointed out by Korty et al. (2008), elevated $CO_2$ is insufficient, to reduce the planetary temperature gradient to the low gradients found during equable climates (e.g., Barron and Washington, 1985; Sloan and Rea, 1996; Shellito et al., 2003).~~ In order to mimick the effect of a higher effective heat capacity and deepened mixed layer depth, the vertical mixing coefficient is increased in the ocean, changing the values for the background vertical diffusivity (arbritarily) by a factor of ~~25. The~~ 25, providing a deeper thermocline. The mixing has a background value plus a mixing process strongly influenced by the shears of the mean currents. Although observations give a range of values of $k_v$ for the ocean interior, models use simplified physics and prescribe a constant background value. The model uses a classical vertical eddy viscosity and diffusion scheme (Pacanowski and Philander, 1981). ~~The orbital~~ Orbital parameters are fixed to the present condition. ~~The changed vertical mixing coefficients are mimicking possible effects like weak tidal dissipation or abyssal stratification (e.g., Green and Huber, 2013), but its explicit physics is not evaluated here.~~

Fig. 9 shows the anomalous near surface temperature for the new vertical mixing experiment relative to the control climate (Wei and Lohmann, 2012). Both simulations were run over 1000 years of integration in order to receive a quasi-equilibrium at the surface. The differences are related to the last 100 years of the simulation. In the vertical mixing experiment $k_v$ was enhanced ~~(factor of 25 is related to a $\sim$ 5 times deeper thermocline according to (16))~~ leading to more heat ~~uptake~~ is taken up by the ocean ~~and~~ producing equable climates with pronounced warming at polar latitudes (Fig. 9~~, in a similar way as in the EBM (Fig. 7).~~). Heat gained at the surface is diffused down the water column, and, compared to the control simulation, the wind-induced Ekman cells in the upper part of the oceans intensified and deepened. Furthermore, the model indicates that the respective winter signal of high-latitude warming is most pronounced (Fig. 9), decreasing the seasonality, ~~also consistent with~~ suggesting a common signal of pronounced warming and weaker seasonality, a feature already seen in our EBM (Fig. 8~~.~~).

~~The surface warming is highest at high latitudes because of the disappearance of sea ice and effective buffering of the summer heating in the surface water.Interestingly,~~

Previous studies have noted that changing the ocean mixed layer depth impacts the climatological annual mean temperature (Schneider and Zhu, 1998; Qiao et al., 2004; Donohoe et al., 2014; Wang et al., 2019). The increased heat capacity of the mixed layer reduced the magnitude of the ~~surface temperature distribution bears similarities with Paleogene/Neogene climate change (e.g.,~~ annual cycle affecting the surface winds and upwelling which may provide non-linear effects (Wang et al., 2019). For the past, a strong warming at high latitudes is reconstructed for the Pliocene, Miocene, Eocene periods (Markwick, 1994; Wolfe, 1994; Sloan and Rea, 1996; Huber et al., 2000; Shellito et al., 2003; Tripati et al., 2003; Mosbrugger et al., 2005; Utescher and Mosbrugger, 2007). It is a conundrum that the modelled high latitudes are not as warm as the reconstructions (e.g., Sloan and Rea, 1996; Huber et al., 2000; Mosbrugger et al., 2005; Knorr et al., 2011; Dowset et al., 2013). The low latitude warming is only moderate. Inspired by the EBM and GCM results, we may think of a climate system having a higher effective heat capacity producing a reduced seasonal cycle and flat temperature gradients. The changed vertical mixing coefficients are mimicking possible effects like weak tidal dissipation or abyssal stratification (e.g., Lambeck 1977; Green and Huber, 2013), but its explicit physics is not evaluated here. ~~Those published temperature patterns resemble the high latitude warming (with moderate low latitude warming) structures suggesting a common mechanism in the modeled and reconstructed temperature patterns. Note,~~

that the modelled Paleogene/Neogene warming is more intense in winter temperature than in summer temperature (Figs.7, 9).
It might be that the more effective mixing provides an explanation that high latitudes were much warmer than present and more equable in that the summer-to-winter range of temperature was much reduced (Sloan and Barron, 1990, Valdes et al., 1996; Sloan et al., 2001; Spicer et al. 2004).

There is a range of literature on the parameterisations of vertical mixing in ocean circulation models (e.g., Mellor and Yamada, 1974; Philander and Pacanowksi, 1981; Luyten et al., 1983; Large et al., 1994) and a detailed discussion is not given here. The mixing has a background value plus a mixing process strongly influenced by the shears of the mean currents. Although observations give a range of values of $k_v$ for the ocean interior, models use simplified physics and prescribe a constant background value. In numerical modelling, the values are also constrained by the required numerical stability and to fill gaps left by other parameterisations (e.g., Griffies, 2005) . $k_v$ largely determines the intensity of the diabatic processes and thus influence the meridional mass transport (Bryan, 1987) affecting the large-scale ocean circulation and its sensitivity (Scott and Marotzke, 2002; Prange Interestingly, it has been suggested that the tight link between ocean temperature and $CO_2$ formed only during the Pliocene when the thermocline shoals and surface water became more sensitive to $CO_2$ (La Riviere et al., 2012) which is therefore of major importance for the understanding of the climate-carbon cycle (Wiebe and Weaver, 1999; Zachos et al., 2003; Rahmstorf et al., 2006; Green and Huber, 2013; De 2008; de Boer and Hogg, 2014; de Lavergne et al., 2016; Hutchinson et al., 2018). Lambeck (1977) calculated the total rate of energy dissipation based on the numerical tide model, indicating a dominant role of ocean continent geometry and sea floor topography. Visser (2007) discussed potential biomixing in the oceans and concluded that the mixing efficiency of small organisms is extremely low. Most of the mechanical energy they impart to the oceans isdissipated almost immediately as heat. There may be a case to be made for biomixing by larger animals on a local scale, but their relatively low abundance means that they are unlikely to be important contributors to global circulation. It has to be explored if the marine organisms could have been different in the distant past in order to introduce significant changes in mixing. As a next step, one can change the large-scale ocean gateways and changed orography/topography in order to realistically simulate past climates and to separate potential forcing factors. ).

## 6 Conclusions

Energy balance models estimate the changes in the climate system from an analysis of

This manuscript revisits the relationship between the (global mean) surface temperature of the Earth and its radiation budget as is frequently used in Energy balance models (EBMs). The main point is, that the effective heat capacity and its temporal variation over the daily/seasonal cycle needs to be taken into account when estimating surface temperature from the energy budgetof the Earth. In their simplest form, they do not include any explicit spatial dimension, providing only globally averaged values for the computed variables. Energy balance models . EMBs provide a crucial tool in climate research, especially because they - confirmed by the results of the elaborate realistic climate models - describe the processes essential for the genesis of the global climate. EBMs are thus an admissible conceptual tools, due to its reduced complexity to the essentials "scientific understanding" represents (von Storch et al., 1999). This understanding states that the radiation balance on the ground and

the absorption in the atmosphere are the essential factors for determining the temperature. Eq. (3) says that the temperature is independent of the size of the Earth and the thermal characteristics, but depends on the albedo, emissivity and solar constant.

The argument follows the ~~1st~~ 1$^{st}$ law of thermodynamics on the conservation of energy: in steady state the Earth has to emit as much energy as it receives from the Sun. However, I argue that we shall explicitly emphasize the Earth as a rapidly rotating object with a significant heat capacity in our EBMs. Without these effects, the global mean temperature would be ~~in the order of 163 K.~~much lower. This description can be better used for objects like the Moon or Mercury (Vasavada et al., 1999) as slowly rotating bodies without significant heat capacity. The Earth system understanding says that these effects are important for the radiation balance, other processes - like horizontal transport processes - are only of secondary importance for the globally averaged temperature. The linearization of the long wave radiation in several models (North et al., 1975a, b; Chen et al., 1995) implicitely assumes the above heat capacity and fast rotation arguments. ~~This linearization is different from the remarkable linear outgoing longwave radiation with respect to T due to the water vapor greenhouse effect (Koll and Cronin, 2018). Model scenarios in conjunction with long-term data can be used to examine mechanisms for climate change under different boundary conditions (for an overview: IPCC 2013).~~ Ironically, the global mean temperature in the revised EBM is very close to the original proposed value. ~~It can be speculated that most findings dealing with climate sensitivity, the change in global temperature when changing $CO_2$, are robust.~~

As a basic feature, we detect the strong dependence of the temperature distribution on the effective heat capacity linked to the mixed-layer depth. A change in the mixed layer depth which likely happened through glacial-interglacial cycles (e.g. Zhang et al., 2014) ~~is~~ can therefore an important driver constraining climate sensitivity (Köhler, et al., 2010). This could be also relevant for future climate change when the ocean stratification can change. ~~It would be interesting to include a temperature-dependent emissivity as e.g. in Dijkstra and Viebahn (2015).~~

~~As a key aspect for climate sensitivity, La Riviere et al. (2012) have claimed that the tight link between ocean temperature and $CO_2$ formed only during the Pliocene when the thermocline shoals and surface water became more sensitive to $CO_2$ which is therefore of major importance for the understanding of the climate-carbon cycle (Wiebe and Weaver, 1999; Zachos et al., 2008; de Boer and Hogg, 2014). Schwartz (2007) stressed out that the effective heat capacity is not an intrinsic property of the climate system but is reflective of the rate of penetration of heat energy into the ocean in response to the particular pattern of forcing and -as suggested by La Riviere et al. (2012)- also to the background state. As one application, we change the vertical mixing in the ocean affecting the effective heat capacity. The resulting temperature might explain the long-lasting question of a low equator-to-pole gradients during the Paleogene/Neogene climate (Markwick, 1994; Wolfe, 1994; Sloan and Rea, 1996; Huber et al., 2000; Shellito et al., 2003; Tripati et al., 2003; Mosbrugger et al., 2005). It is~~ It is concluded that climate studies should use improved representations of vertical mixing processes including turbulence, tidal mixing, hurricanes and wave breaking (e.g., Qiao et al., 2004; Huber et al., 2004; Simmons et al., 2004; Korty et al., 2008; Griffiths and Peltier, 2009; Green and Huber, 2013; Reichl and Hallberg, 2018). ~~It could be that the climate models have to be de-tuned.Korty et al.(2008)explore this issue with a parameterization coupling upper tropical mixing to tropical cyclone activity.~~Global climate models treat ocean vertical mixing as static, although there is little reason to suspect this is correct (e.g., see Munk and Wunsch, 1998). In numerical modelling, the values are also constrained by the required numerical stability and to fill gaps left by other

parameterisations (e.g., Griffies, 2005). As a natural next step, one ~~can analyze the climate-dependent heat transport due to baroclinic instability in the atmosphere (Stone and Yao, 1990; Fu~~ shall analyze the ocean mixing/heat uptake (Luyten et al., 1983; Large et al., 1994~~) and ocean mixing/heat uptake (~~; Nilsson, 1995~~; Munk and Wunsch, 1998; Wunsch and Ferrari, 2004; Olbers and Eden, 2017) )~~ to understand past, present and future temperatures.

*Acknowledgements.* Thanks go to Peter Köhler~~and Dirk Olbers~~, Dirk Olbers, and anonymous referees for comments on earlier versions of the manuscript. Madlene Pfeiffer and Christian Stepanek are acknowledged for their contribution in producing Fig. 7. This work was funded by the Helmholtz Society through the research program PACES.

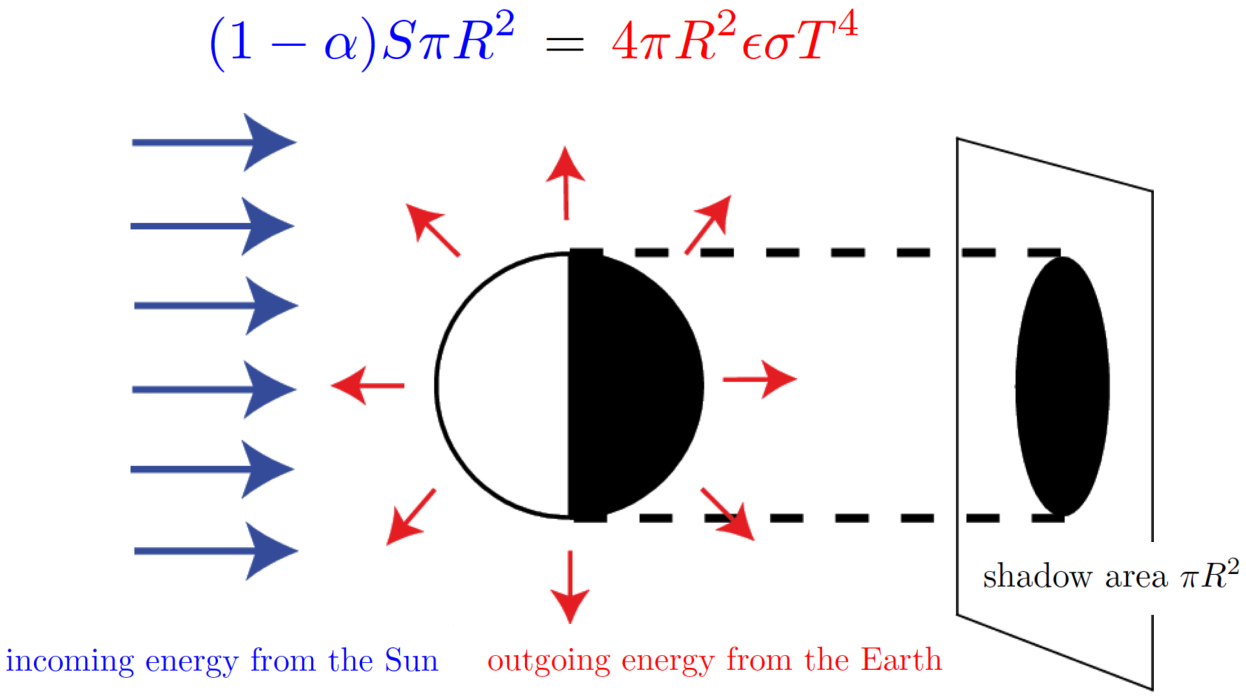


**Figure 1.** Schematic view of the energy absorbed and emitted by the Earth following (1). Modified after Goose (2015).

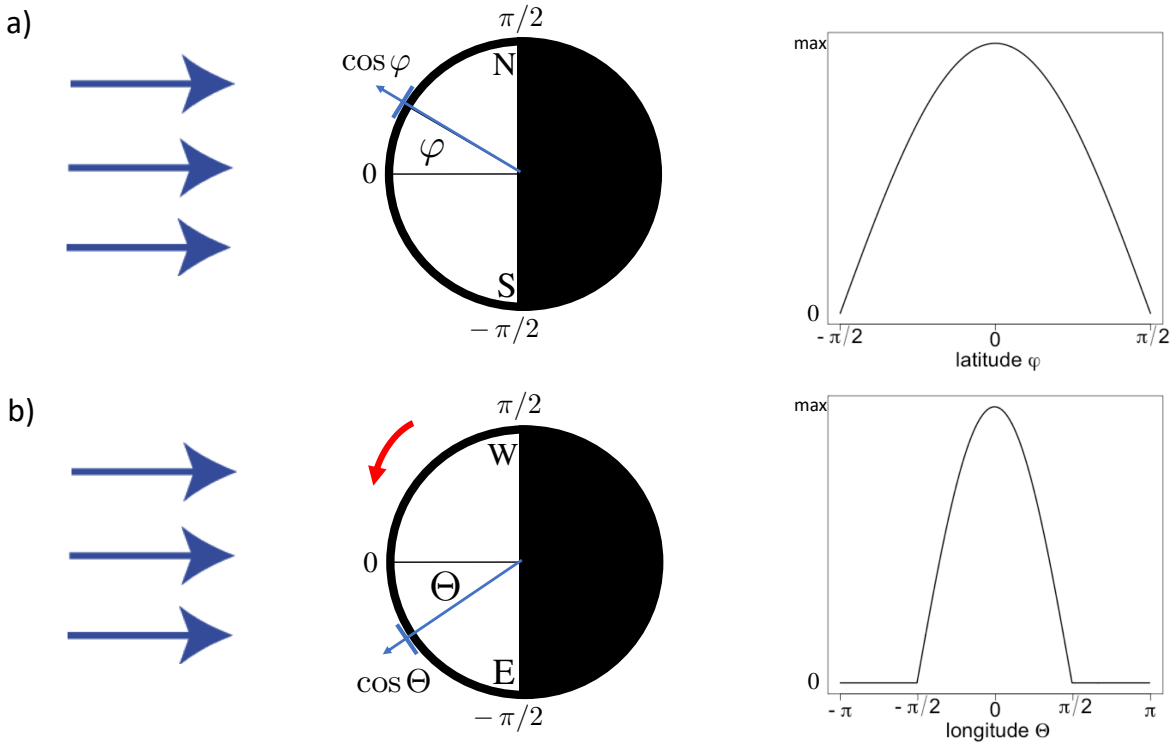


**Figure 2.** Latitudinal (a) and longitudinal (b) dependence of the incoming short wave radiation. On the right hand side, the insolation as a function of latitude $\varphi$ and longitude $\Theta$ with maximum insolation $(1-\alpha)S$ is shown. See text for the details.

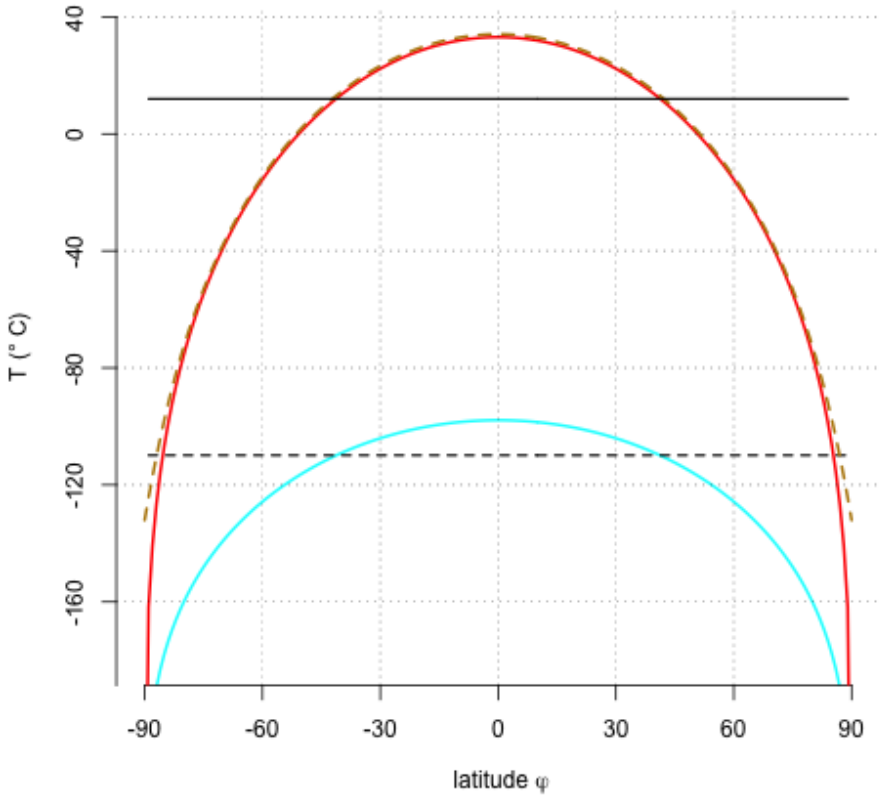


**Figure 3.** Latitudinal temperatures of the EBM with zero heat capacity (7) in cyan (its mean as a dashed line), the global approach (3) as solid black line, and the zonal and time averaging (11) in red. The dashed brownish curve shows the numerical solution by taking the zonal mean of (9).

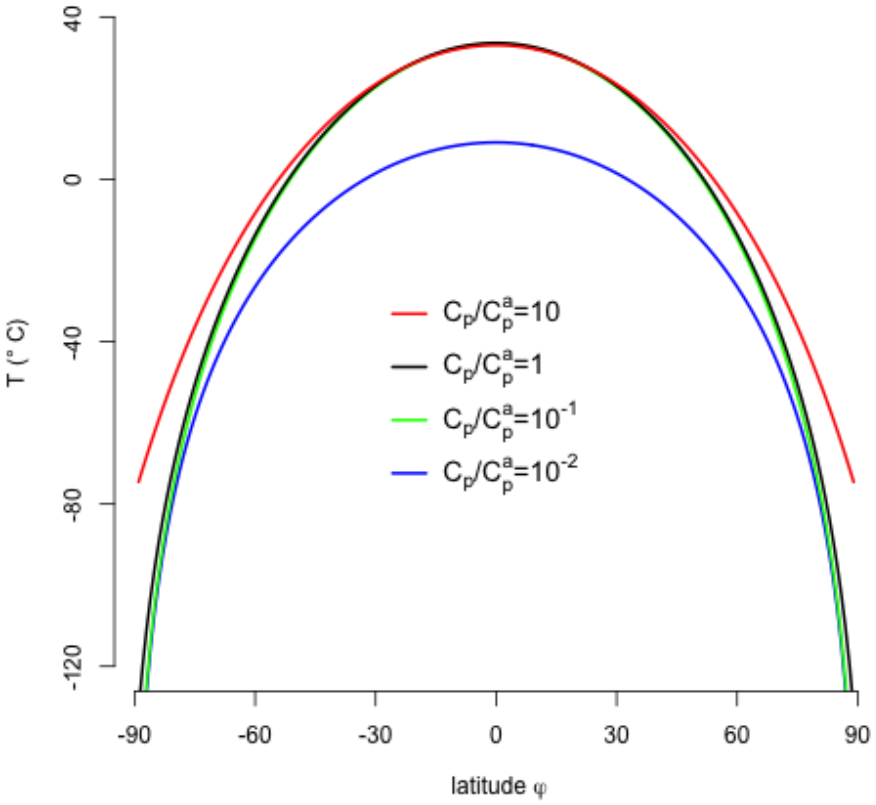


**Figure 4.** Temperature depending on $C_p$ when solving (9) numerically. The reference heat capacity is the atmospheric heat capacity $C_p^a = 1.02 \cdot 10^7 JK^{-1}m^{-2}$. The climate is insensitive to changes in heat capacity $C_p \in [0.05 \cdot C_p^a, 2 \cdot C_p^a]$.

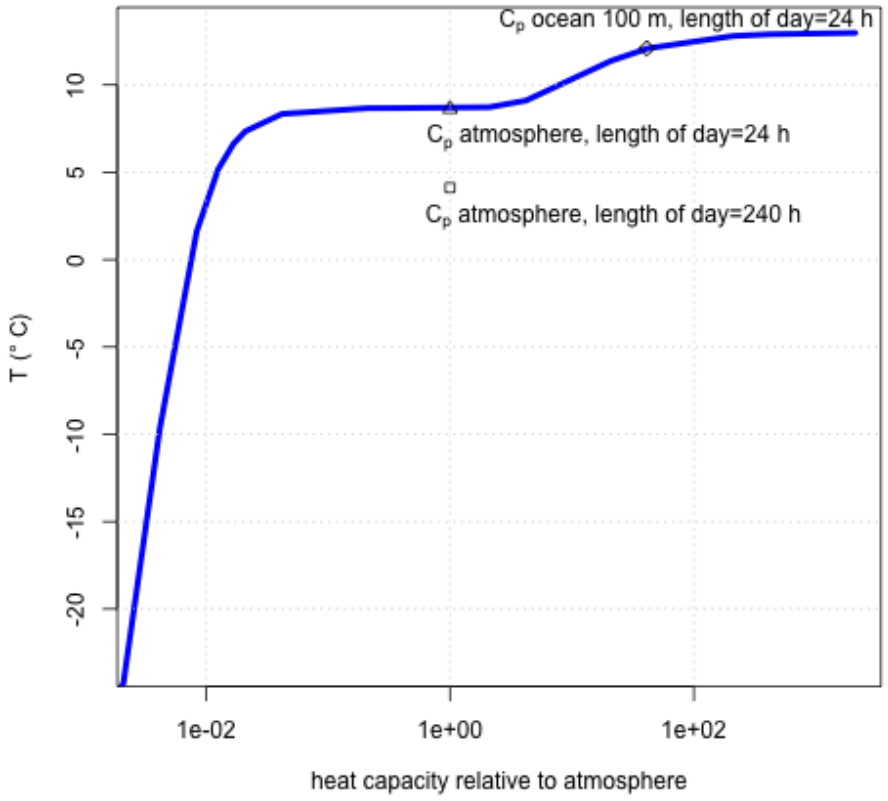


**Figure 5.** Temperature dependence on heat capacity (and rotation rate) when analyzing the diurnal cycle at 45°.

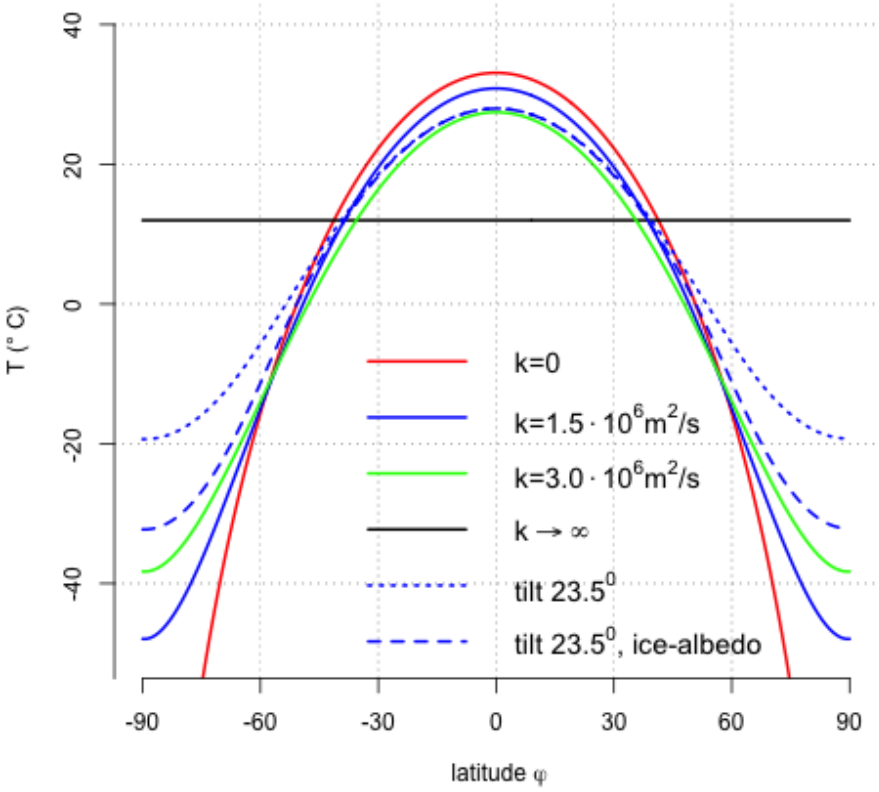


**Figure 6.** Equilibrium temperature of (13) using different diffusion coefficients. $C_p = C_p^a$. The blue lines use $1.5 \cdot 10^6 m^2/s$ with no tilt (solid line), a tilt of $23.5^\circ$ (dotted line), and as the dashed line a tilt of $23.5^\circ$ (present value) and ice-albedo feedback using the respresentation of Sellers (1969). Except for the dashed line, the global mean values are identical to the value calculated in (12). Units are $^\circ$C.

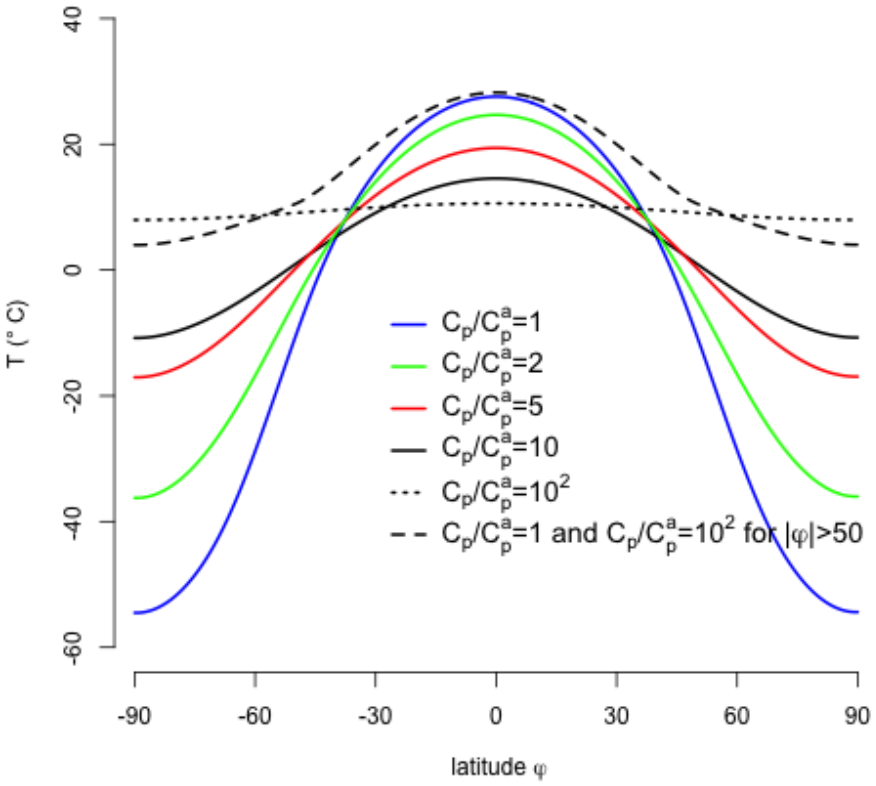


**Figure 7.** Annual mean temperature depending on $C_p$ when solving the seasonal resolved EBM (14) numerically. For all solutions, we use use $k = 1.5 \cdot 10^6 m^2/s$, present day orbital parameters, and the ice-albedo feedback using the respresentation of Sellers (1969).

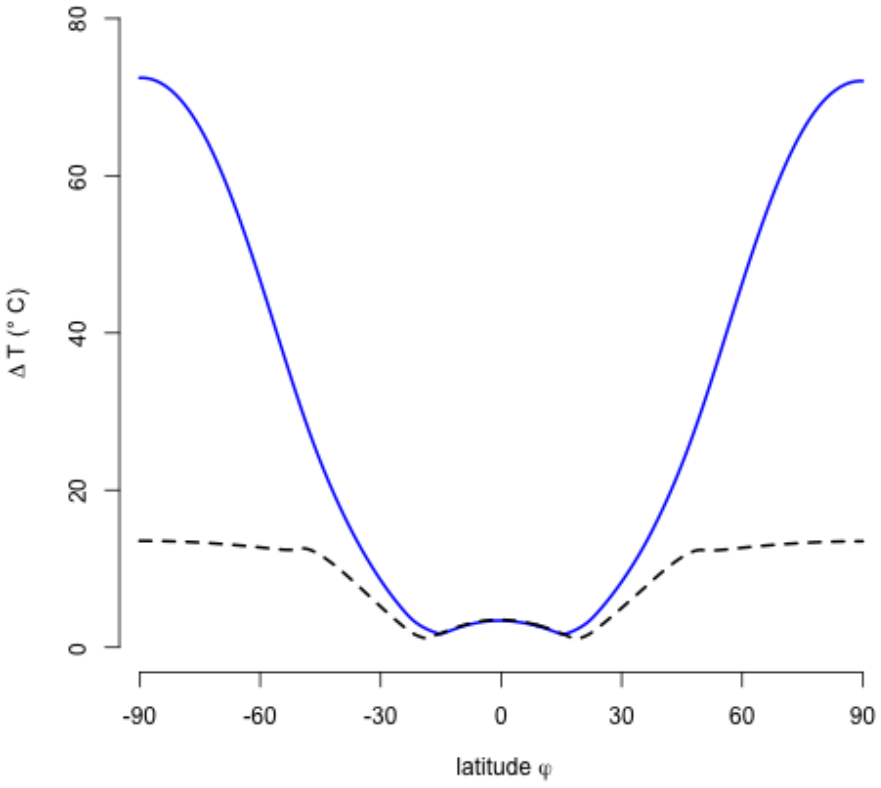


**Figure 8.** Seasonal amplitude of temperature for the two extreme scenarios in Fig. 7, indicating that a lower seasonality dashed-black relative to the blue line is linked to warmer annual mean climate.

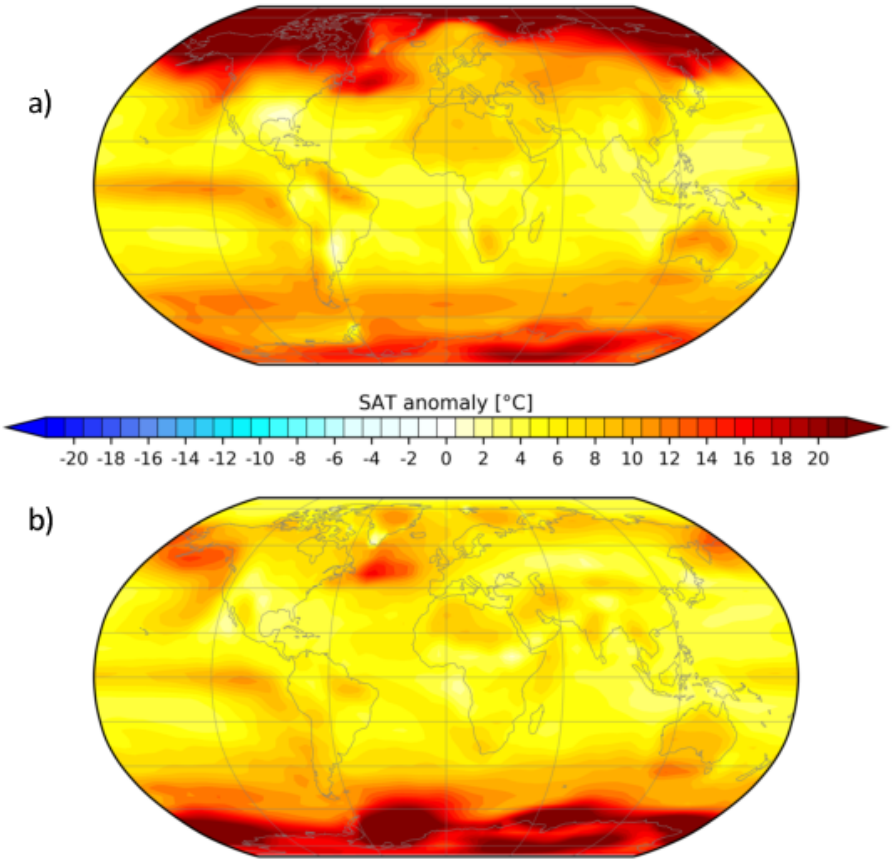


**Figure 9.** Anomalous near surface temperature for the vertical mixing experiment relative to the control climate. a) Mean over boreal winter and austral summer (DJF), b) Mean over austral winter and boreal summer (JJA). Shown is the 100 year mean after 900 years of integration using the Earth system model COSMOS. Units are °C.

## References


Adem, J.: Experiments Aiming at Monthly and Seasonal Numerical Weather prediction. Mon. Weather Rev. 93,495-503, 1965.

Adem, J.: Numerical simulation of the annual cycle of climate during the ice ages, J. Geophys. Res., 86, 12015-12034, 1981.

Anderson S.P., Weller, R.A., and Lukas, R.B.: Surface buoyancy forcing and the mixed layer of the western pacific warm pool: observations and 1D model results. J~~Clim~~ . Clim. 9:3056-3085, 1996.

Archer, D.: Global Warming: Understanding the Forecast. ISBN: 978-1-4443-0899-0. 288 pages, Wiley-Blackwell, 2009.

Berger, A., and Loutre, M.F.: Insolation values for the climate of the last 10 million years, Quat. Sci. Rev., 10(4), 297 - 317, 1991.

Berger, A., and Loutre, M.F.: Intertropical latitudes and precessional and half-precessional cycles, Science, 278(5342), 1476 - 1478, 1997.

~~Bryan, F.: Parameter sensitivity of primitive equation ocean general ciculation models. J. Phys. Oceanogr. 17, 970-985, 1987.~~

Budyko, M.I.: The effect of solar radiation variations on the climate of the Earth. Tellus 21,611-619, 1969.

Chen, D., Gerdes, R., and Lohmann, G.: A 1-D Atmospheric energy balance model developed for ocean modelling. Theor. Appl. Climatol. 51, 25-38, 1995.

Claussen, M., Mysak, L.A., Weaver, A.J., Crucifix, M., Fichefet, T., Loutre, M.-F., Weber, S.L., Alcamo, J.,Alexeev, V.A., Berger, A., Calov, R., Ganopolski, A., Goosse, H., Lohmann, G.,Lunkeit, F., Mokhov, I.I., Petoukhov, V., Stone, P., and Wang, Z.: Earth System Models of Intermediate Complexity: Closing the Gap in the Spectrum of Climate System Models. Climate Dynamics 18, 579-586, 2002.

de Boer, A. M. and Hogg, A. M.: Control of the glacial carbon budget by topographically induced mixing, Geophys. Res. Lett., 41, 4277-4284, 2014.

de Boyer Montégut C., Gurvan M., and Fischer A. S.: Mixed layer depth over the global ocean: an examination of profile data and a profilebased climatology. Journal of Geophysical Research: Oceans, 109 (C12): C12003, 2004.

~~Dijkstra, H.A., and Viebahn, J. P.: Sensitivity and resilience of the climate system: A conditional nonlinear optimization approach. Communications in Nonlinear Science and Numerical Simulation, 22(1-3): 13-22, 2015.~~

~~de Lavergne, C., Madec, G., Le Sommer, J., Nurser, A.J. G., and Naveira Garabato, A.C~~Donohoe A., Frierson D.M.W., and Battisti D.S.: The ~~Impact of a Variable Mixing Efficiency on the Abyssal Overturning, J. Phys. Oceanogr. , 46, 663-681, https://doi.org/10.1175/JPO-D-14-0259.1, 2016.~~ effect of ocean mixed layer depth on climate in slab ocean aqua-planet experiments. Clim. Dyn. 43(3-4):1041?1055, 2014.

Dowsett, H. J. , K. M. Foley, D. K. Stoll, M. A. Chandler, L. E. Sohl, M. Bentsen, B. L. Otto-Bliesner, F. J. Bragg, W.-L. Chan, C. Contoux, A. M. Dolan, A. M. Haywood, J. A. Jonas, A. Jost, Y. Kamae, G. Lohmann, D. J. Lunt , K. H. Nisancioglu, A. Abe-Ouchi, G. Ramstein, C. R. Riesselman, M. M. Robinson, N. A. Rosenbloom, U. Salzmann, C. Stepanek, S. L. Strother, H. Ueda, Q. Yan, Z. Zhang: Sea Surface Temperature of the mid-Piacenzian Ocean: A Data-Model Comparison. Scientific Reports 3; Article number: 2013; DOI:10.1038/srep02013, 2013.

Fanning, A.F., and Weaver, A. J.: An atmospheric energy-moisture balance model: Climatology, interpentadal climate change, and coupling to an ocean general circulation model. J. Geophys. Res. 101 (D10), 15111-15128, 1996.

Fu, R., Del Genio, A.D., and Rossow, W.B.: Influence of ocean surface conditions on atmospheric vertical thermodynamic structure and deep convection. J. Climate, 7, 1092-1107, 1994.

Ghil, M.: Climate stability for a Sellers-type model. J. Atmos. Sci., 33, 3-20, 1976.

Ghil, M, and Childress, S.: Topics in geophysical fluid dynamics: atmospheric dynamics, dynamo theory, and climate dynamics. New York, NY: Springer, 1987.

Ghil, M.: Climate stability for a Sellers-type model. J. Atmos. Sci., 33, 3-20, 1976.

Green, J.A.M., and Huber, M.: Tidal dissipation in the early Eocene and implications for ocean mixing, Geophys. Res. Lett., 40, 2707?2713, doi:10.1002/grl.50510, 2013.

Griffies, S.M.: Fundamentals of Ocean Climate Models. Princeton University Press, Princeton, USA. ISBN9780691118925 528 pp, 2005.

Griffiths, S.D., and Peltier, W.R.: Modeling of Polar Ocean Tides at the Last Glacial Maximum: Amplification, Sensitivity, and Climatological Implications. Journal of Climate J. Clim. 22, 2905-2924, 2009.

Goosse, H.: Climate system dynamics and modelling. Cambridge University Press, ISBN: 9781107445833, 2015.

Hansen, J., Ruedy, R., Sato, M., and Lo, K.: Global surface temperature change. Rev. Geophys., 48, RG4004, doi:10.1029/2010RG000345, 2010.

Hardy, G. H., Littlewood, J. E., Pólya, G.: Inequalities. 1934. Cambridge University Press, pp. 314, ISBN 0-521-35880-9, JFM 60.0169.01

Hartmann, D. L., Global Physical Climatology, Academic Press, 1994.

Hasselmann, K.: Stochastic climate models. Part I, Theory. Tellus, 6:473–485, 1976.

Hölder, O.: Ueber einen Mittelwertsatz. Nachrichten von der Königl. Gesellschaft der Wissenschaften und der Georg-Augusts-Universität zu Göttingen, 2, 38-47, 1889.

Huber, B.T., MacLeod, K.G., and Wing, S.L. (Eds.): Warm Climates in Earth History. Cambridge University Press, 462 pp, 2000.

Huber, M., H. Brinkhuis, C. E. Stickley, K. Doos, A. Sluijs, J. Warnaar, G. L. Williams, and S. A. Schellenberg: Eocene circulation of the Southern Ocean: Was Antarctica kept warm by subtropical waters?, Paleoceanography, 19, PA4026, doi:10.1029/2004PA001014, 2004.

Hutchinson, D. K., A. M. de Boer, H. K. Coxall, R. Caballero, J. Nilsson, and M. Baatsen: Climate sensitivity and meridional overturning circulation in the late Eocene using GFDL CM2.1. Clim. Past, 14, 789-810, 2018.

IPCC: Climate Change: The Physical Science Basis. Contribution of Working Group I to the Fifth Assessment Report of the Intergovernmental Panel on Climate Change Stocker, T.F., D. Qin, G.-K. Plattner, M. Tignor, S.K. Allen, J. Boschung, A. Nauels, Y. Xia, V. Bex and P.M. Midgley (eds.). Cambridge University Press, Cambridge, United Kingdom and New York, NY, USA, 1535 pp, 2013.

Jungclaus, J. H., Lorenz, S. J., Timmreck, C., Reick, C. H., Brovkin, V., Six, K., Segschneider, J., Giorgetta, M. A., Crowley, T. J., Pongratz, J., Krivova, N. A., Vieira, L. E., Solanki, S. K., Klocke, D., Botzet, M., Esch, M., Gayler, V., Haak, H., Raddatz, T. J., Roeckner, E., Schnur, R., Widmann, H., Claussen, M., Stevens, B., and Marotzke, J.: Climate and carbon-cycle variability over the last millennium, Clim. Past, 6, 723-737, 2010.

Kawai, Y., and Kawamura, H.: Evaluation of the diurnal warming of sea surface temperature using satellite derived marine meteorological data. J Oceanogr 58:805-814, 2002.

Knorr, G., Butzin, M., Micheels, A., and Lohmann, G.: A Warm Miocene Climate at Low Atmospheric $CO_2$ levels. Geophysical Research Letters, L20701, doi:10.1029/2011GL048873, 2011.

Knorr, G., and Lohmann, G.: A warming climate during the Antarctic ice sheet growth at the Middle Miocene transition. Nature Geoscience, 7, 376-381, 2014.

Köhler, P., Bintanja, R., Fischer, H., Joos, F., Knutti, R., Lohmann, G., and Masson-Delmotte, V.: What caused Earth's temperature variations during the last 800,000 years? Data-based evidence on radiative forcing and constraints on climate sensitivity. Quaternary Science Reviews 29, 129-145. doi:10.1016/j.quascirev.2009.09.026, 2010.

Koll, D. D. B., and Cronin, J. R.: Earth's outgoing longwave radiation linear due to $H_2O$ greenhouse effect. Proceedings National Academy of Sciences, 115 (41) 10293-10298, 2018.

Korty, R. L, Emanuel, A. K. A., and Scott, J. R.: Tropical Cyclone-Induced Upper-Ocean Mixing and Climate: Application to Equable Climates. J. Climate, 21, 638-654, 2008.

Kuptsov, L. P.: Hölder inequality. In Hazewinkel, Michiel (ed.), Encyclopedia of Mathematics, Springer Science+Business Media B.V. / Kluwer Academic Publishers, ISBN 978-1- 55608-010-4, 2001.

Laepple, T., and Lohmann, G.: The seasonal cycle as template for climate variability on astronomical time scales. Paleoceanography, 24, PA4201, doi:10.1029/2008PA001674, 2009.

Lambeck, K.: Tidal dissipation in the oceans: astronomical, geophysical and oceanographic consequences Phil. Trans. R. Soc. Lond. A, 287, 545-594, 1977.

Large, W.G., McWilliams, J.C., and Doney, S.C.: Oceanic vertical mixing: a review and a model with a nonlocal boundary layer parameterization Rev. Geophys., 32 (4), 363-403, 1994.

Lemke, P.: Stochastic climate models, part 3. Application to zonally averaged energy models, Tellus, 29:5, 385-392, 1977.

La Riviere, J.P., Ravelo, A.C., Crimmins, A., Dekens, P.S., Ford, H.L., Lyle, M., Wara, M.W.: Late Miocene decoupling of oceanic warmth and atmospheric carbon dioxide forcing. Nature 486, 97-100, 2012.

Le Treut, H., R. Somerville, U. Cubasch, Y. Ding, C. Mauritzen, A. Mokssit, T. Peterson and M. Prather: Historical Overview of Climate Change. In: Climate Change 2007: The Physical Science Basis. Contribution of Working Group I to the Fourth Assessment Report of the Intergovernmental Panel on Climate Change [Solomon, S., D. Qin, M. Manning, Z. Chen, M. Marquis, K.B. Averyt, M. Tignor and H.L. Miller (eds.)]. Cambridge University Press, Cambridge, United Kingdom and New York, NY, USA, 2007.

Lohmann, G.: ESD Ideas: The stochastic climate model shows that underestimated Holocene trends and variability represent two sides of the same coin. Earth Syst. Dynam. 9, 1279-1281, 2018.

Lohmann, G., Pfeiffer, M., Laepple, T., Leduc, G., and Kim, J.-H.: A model-data comparison of the Holocene global sea surface temperature evolution. Clim. Past, 9, 1807-1839, 2013.

Lohmann, G., Gerdes, R., and Chen, D.: Sensitivity of the thermohaline circulation in coupled oceanic GCM-atmospheric EBM experiments. Climate Dynamics 12, 403-416, 1996.

Lohmann, G., and Gerdes, R.: Sea ice effects on the Sensitivity of the Thermohaline Circulation in simplified atmosphere-ocean-sea ice models. J. Climate 11, 2789-2803, 1998.

Luyten, J., Pedlosky, J., and Stommel, H.: The ventilated thermocline. J. Phys. Oceanogr., 13, 292-309, 1983.

Markwick, P.J.: 'Equability', continentality and Tertiary 'climate': the crocodilian perspective. Geology, 22, 613-616, 1994.

~~Mellor, G. L. and Yamada, T.: A Hierarchy of Turbulence Closure Models for Planetary Boundary Layers. Journal of Atmospheric Sciences 31 (7), 1791-1806, 1974.~~

Mosbrugger, V., Utescher, T. , and D. L. Dilcher: Cenozoic continental climatic evolution of Central Europe. Proceedings National Academy of Sciences, 102: 14964-14969, 2005.

Munk, W., and Wunsch, C.: Abyssal recipes II: Energetics of tidal and wind mixing. Deep-Sea Res., 45, 1977-2010, 1998.

Nilsson, J.: Energy flux from traveling hurricanes to the oceanic internal wave field. J. Phys. Oceanogr., 25, 558-573, 1995.

North, G. R.: Analytical solution of a simple climate model with diffusive heat transport. J. Atm. Sci. 32, 1300-1307, 1975a

North, G. R.: Theory of energy-balance climate models. J. Atm. Sci. 32, 2033-2043, 1997b.

North G.R., Cahalan R.F., Coakley J.A.: Energy balance climate models. Rev. Geophys. Space Phys. 19, 91-121, 1981.

North G.R., Mengel, J.G., Short D.A.: Simple energy balance model resolving the seasons and the continents: application to the astronomical theory of the ice ages. J. Geophys. Res. 88, 6576-6586, 1983.

North, G. R., and Kim, K.-Y.: Energy Balance Climate Models. Wiley, 2017. ISBN:9783527411320, DOI:10.1002/9783527698844

Olbers, D.J., Wenzel, M., and Willebrand, J.: The inference of North Atlantic circulation patterns from climatological hydrographic data. Rev. Geophys. 23(4), 313-356, 1985.

Olbers, D., and Eden, C.: A closure for internal wave-mean flow interaction. Part II: Wave drag. Journal of Physical Oceanography 47 (6), 1403-1412, 2017.

Pacanowski, R. C., and Philander, S. G. H.: Parameterization of Vertical Mixing in Numerical Models of Tropical Oceans. J. Phys. Oceanogr. 11, 83-89, 1981.

Peixoto, J. P., and Oort, A. H.: Physics of Climate, ISBN-13: 978-0883187128, ISBN-10: 0883187124, AIP Press, Springer Verlag, Berlin Heidelberg, New York, 1992.

Pfeiffer, M., and Lohmann, G.: Greenland Ice Sheet influence on Last Interglacial climate: global sensitivity studies performed with an atmosphere-ocean general circulation model, Clim. Past, 12, 1313-1338, 2016.

Pierrehumbert, R.T.: Principles of Planetary Climate. Cambridge University Press. Online ISBN: 9780511780783 DOI:10.1017/CBO9780511780783, 2010.

Prange, M. , Lohmann, G., and A. Paul: Influence of vertical mixing on the thermohaline hysteresis: Analyses of an OGCM. J. Phys. Oceanogr., 33 (8), 1707-1721, 2003.

Qiao, F., Yuan, Y., Yang, Y., Zheng, Q., Xia, C., and Ma, J.: Wave-induced mixing in the upper ocean: Distribution and application to a global ocean circulation model Geophysical Research Letters 31 (11), https://doi.org/10.1029/2004GL019824, 2004.

Rahmstorf, S., M. Crucifix, A. Ganopolski, H. Goosse, I. Kamenkovich, R. Knutti, G. Lohmann, B. Marsh, L. A. Mysak, Z. Wang, A. Weaver, 2005: Thermohaline circulation hysteresis: a model intercomparison. Geophys. Res. Lett., 32, L23605, doi:10.1029/2005GL023655.

Reichl, B.G., and Hallberg, R.: A simplified energetics based planetary boundary layer (ePBL) approach for ocean climate simulations. Ocean Modelling 132, 112-129, 2018.

Rogers, L. J.: An extension of a certain theorem in inequalities. Messenger of Mathematics, New Series, XVII (10): 145?150, 1888. JFM 20.0254.02

Ruddiman, W.F.: Earth's Climate: Past and Future. W H Freeman & Co, 354 pages, ISBN-13: 978-0716737414, 2001.

Saltzman, B.: Dynamical Paleoclimatology: Generalized Theory of Global Climate Change. ISBN-13: 978-0123971616, ISBN-10: 0123971616, 2001.

Schneider, E.K., Zhu, Z.: Sensitivity of the simulated annual cycle of sea surface temperature in the equatorial Pacific to sunlight penetration. J. Clim. 11, 1932-1950, 1998.

Schwartz, S.E.: Heat capacity, time constant, and sensitivity of Earth's climate system. J Geophys Res 112: D24S05, doi:10.1029/2007JD008746, 2007.

Scott, J. R., and Marotzke, J.: The location of diapycnal mixing and the meridional overturning circulation. J. Phys. Oceanogr., 32, 3328-3345, 2002.

Sellers, W. D.: A global climate model based on the energy balance of the earth-atmosphere system. J. Appl. Meteorol. 8, 392-400, 1969.

Sellers, W. D.: A new global climate model. J. Appl. Meteorol. 12, 241-254, 1973.

Shellito, C. J., Sloan, L. C., and Huber, M.: Climate model sensitivity to atmospheric CO2 levels in the early-middle Paleogene. Palaeogeogr. Palaeoclimatol. Palaeoecol., 193, 113-123, 2003.

Short, D. A., J. G. Mengel, T. J. Crowley, W. T. Hyde, and G. R. North: Filtering of Milankovitch Cycles by Earth's Geography. Quaternary Research 35, 2, 157-173, 1991.

Simmons, H. L., Jayne, S. R., Laurent, L. C. S., and Weaver, A. J.: Tidally driven mixing in a numerical model of the ocean general circulation, Ocean Model., 6, 245-263, https://doi.org/10.1016/S1463-5003(03)00011-8, 2004.

Sloan, L. C., and Rea, D. K.: Atmospheric carbon dioxide and early Eocene climate: A general circulation modeling sensitivity study. Palaeogeogr. Palaeoclimatol. Palaeoecol., 119, 275-292, 1996.

Sloan, L.C., and Barron, E.J.: Equable climates during Earth history Geology, 18, 489-492, 1990.

Sloan, L.C., Huber, M., Crowley, T.J., Sewall, J.O., and Baum S.: Effect of sea surface temperature configuration on model simulations of equable climate in the early Eocene Palaeogeogr. Palaeoclimatol. Palaeoecol., 167, 321-335, 2001.

Spicer R.A., Herman, A.B., and Kennedy E.M.: The foliar physiognomic record of climatic conditions during dormancy: CLAMP and the cold month mean temperature J. Geol., 112, 685-702, 2004.

~~Stap, L. B., R. S. W. van de Wal, B. de Boer, P. Köhler, J. H. Hoencamp, G. Lohmann, E. Tuenter, and L. J. Lourens: Modeled influence of land ice and CO2 on polar amplification and paleoclimate sensitivity during the past 5 million years. Paleoceanography and Paleoclimatology, 33 (4), 381-394, 2018.~~

Stein, R., K. Fahl, M. Schreck, G. Knorr, F. Niessen, M. Forwick, C. Gebhardt, L. Jensen, M. Kaminski, A. Kopf, J. Matthiessen, W. Jokat, and G. Lohmann: Evidence for ice-free summers in the late Miocene central Arctic Ocean. Nature comm. 7, 11148, doi:10.1038/ncomms11148, 2016.

Stepanek, C., and Lohmann, G.: Modelling mid-Pliocene climate with COSMOS. Geosci. Model Dev., 5, 1221-1243, 2012.

Stocker, T.: Introduction to Climate Modelling. 182 pp. Springer-Verlag Berlin Heidelberg. doi:10.1007/978-3-642-00773-6 ISBN 978-3-642-00773-6, 2011.

Stocker, T.F., Wright, D.G., and Mysak, L.A.: A zonally averaged, coupled ocean-atmosphere model for paleoclimate studies. J. Climate 5, 773-797, 1992.

Stommel, H., Saunders, K., Simmons, W., and Cooper, J.: Observation of the diurnal thermocline. Deep-Sea Res., 16, 269-284, 1969.

~~Stone, P.H., and Yao, M.S.: Development of a two-dimensional zonally averaged statistical-dynamical model. Part III: The parametrisation of the eddy fluxes of heat and moisture. J. Climate 3,726-740, 1990.~~

Stuart-Menteth, A.C., Robinson, I.S., and Challenor, P.G.: A global study of diurnal warming using satellite-derived sea surface temperature. J Geophys Res 108(C5):3155, 2003.

Su, Q.H., and Hsieh, D.Y.: Stability of the Budyko climate model. J. Atmos. Sci., 33, 2273-2275, 1976.

Tripati, A. K., Delaney, M. L., Zachos, J. C., Anderson, L. D. Kelly, D. C., and Elderfield, H.: Tropical sea-surface temperature reconstruction for the early Paleogene using Mg/Ca ratios of planktonic foraminifera. Paleoceanography, 18, 1101, 2003.

Utescher, T., and Mosbrugger, V.: Eocene vegetation patterns reconstructed from plant diversity - A global perspective. Palaeogeography, Palaeoclimatology, Palaeoecology 247, 243-271, 2007.

Valdes, P.J., Sellwood, B.W., and Price, G.D.: The concept of Cretaceous equability Palaeoclim.: Data Model., 1, 139-158, 1996.

Vasavada, A.R., Paige, D.A., and Wood, S.E.: Near-surface temperatures on Mercury and the Moon and the stability of polar ice deposits. Icarus 141, 179-93, 1999.

~~von der Heydt, A.S., H.A. Dijkstra, R.S.W. van de Wal, R. Caballero, M. Crucifix, G.L. Foster, M. Huber, P. Köhler, E. Rohling, P. J. Valdes, P. Ashwin, S. Bathiany, T. Berends, L. G. J. van Bree, P. Ditlevsen, M. Ghil, A. Haywood, J. Katzav, G. Lohmann, J. Lohmann,~~

V. Lucarini, A. Marzocchi, H. Pälike, I.R. Baroni, D. Simon, A. Sluijs, L.B. Stap, A. Tantet, J. Viebahn, M. Ziegler: Lessons on climate sensitivity from past climate changes. Current Climate Change Reports 2, 148?158. DOI:10.1007/s40641-016-0049-3, 2016.

von Storch, H., Güss, G. S., and Heimann, M.: Das Klimasystem und seine Modellierung: eine Einführung. (in German) Springer-Verlag Berlin Heidelberg. 256pp. doi:10.1007/978-3-642-58528-9, 1999.

Visser, A.W. : Biomixing of the Oceans? Science 316, 5826, 838-839. DOI:10.1126Wang, Z., Schneider, E. K., and Burls, N. J.: The sensitivity of climatological SST to slab ocean model thickness. Climate Dynamics, 1-15, 2019. http:/science.1141272, 2007. /doi.org/10.1007/s00382-019-04892-0

Ward, B.: Near-surface ocean temperature. J Geophys Res 111(C5):1-18. doi:10.1029/2004JC002689, 2006.

Wei, W., and Lohmann, G.: Simulated Atlantic Multidecadal Oscillation during the Holocene. J. Climate, 25, 6989-7002, 2012.

Wiebe, E.C., and Weaver, A. J.: On the sensitivity of global warming experiments to the parameterisation of sub-grid scale ocean mixing. Climate Dyn., 15, 875-893, 1999.

Wolfe, J.A.: Tertiary climatic changes at middle latitudes of western North America. Palaeogeography, Palaeoclimatology, Palaeoecology 108, 195-205, 1994.

Wunsch, C., and Ferrari, R.: Vertical mixing, energy, and the general circulation of the oceans. Annu. Rev. Fluid Mech. 36:281-314, 2004.

Zachos, J.C., Dickens, G.R., and Zeebe, R.E.: An early Cenozoic perspective on greenhouse warming and carbon-cycle dynamics. Nature, 451, 279-283, 2008.

Zhang, X., Lohmann, G., Knorr, G., and Xu, X.: Different ocean states and transient characteristics in Last Glacial Maximum simulations and implications for deglaciation. Clim. Past, 9, 2319-2333, 2013.

Zhang, X., Lohmann, G., Knorr, G., and Purcell, C.: Abrupt glacial climate shifts controlled by ice sheet changes. Nature 512, 290-294, 2014.

# Answer to interactive comment of #referee 1 on Temperatures from Energy Balance Models: the effective heat capacity matters

Gerrit Lohmann[1,2]

[1]Alfred Wegener Institute, Helmholtz Centre for Polar and Marine Research, Bremerhaven, Germany
[2] University of Bremen, Bremen, Germany

Thanks for the constructive critics in the *Interactive comment on Earth Syst. Dynam. Discuss., https://doi.org/10.5194/esd-2019-35, 2019.* by referee #1. In the following, I will repeat and answer to these comments. Furthermore, the actions are described.

**Comment**

This manuscript revisits the relationship between the (global mean) surface temperature of the Earth and its radiation budget as is frequently used in Energy balance models (EBMs). The main point is, that the effective heat capacity (and its temporal variation over the daily/seasonal cycle) needs to be taken into account when estimating surface temperature from the energy budget. The results of this exercise together with coupled ocean-atmosphere GCM simulations lets the author suggest a potential mechanism for the relatively low equator-to-pole temperature gradient in past warm climates that has been observed in proxy data, but remains difficult to reproduce with GCMs. The paper includes a very useful discussion about general properties of the energy balance of the Earth and this certainly justifies publication in ESD. However, I have two main comments to be improved on before I can recommend publication.

**Comment 1a)**

The theoretical arguments should be much better explained. This holds in particular for sections 2 and 3. For example, after or before eq. (4), it should be very explicitly explained which variables become lat-lon dependent, and which not. Otherwise eq. (4) and the analysis that follows is very hard to understand (or reproduce). In my view, if you consider the local energy balance, temperature T, emissivity and albedo $\alpha$, should be spatially dependent and therefore this should have consequences for the following integration. If they are not spatially dependent, then it should be clearly stated why not.

**Answer/Action**

Indeed, eq. (4) can be better explained. I have rewritten section 2, added a figure, and I think the notation is now clearer.

The incoming radiation goes with the cosine of latitude $\varphi$ and longitude $\Theta$, and there is only sunshine during the day. Fig. 1a shows the latitudinal dependence. As we assume no tilt (this assumption is later relaxed), the latitudinal dependence is a function of latitude only: $\cos\varphi$. On the right-hand side, the function is shown. Fig. 1b shows the latitudinal dependence is a function of longitude: $\cos\Theta$ for the sun-shining side of the Earth, and for the dark side of the Earth it is zero. For simplicity,

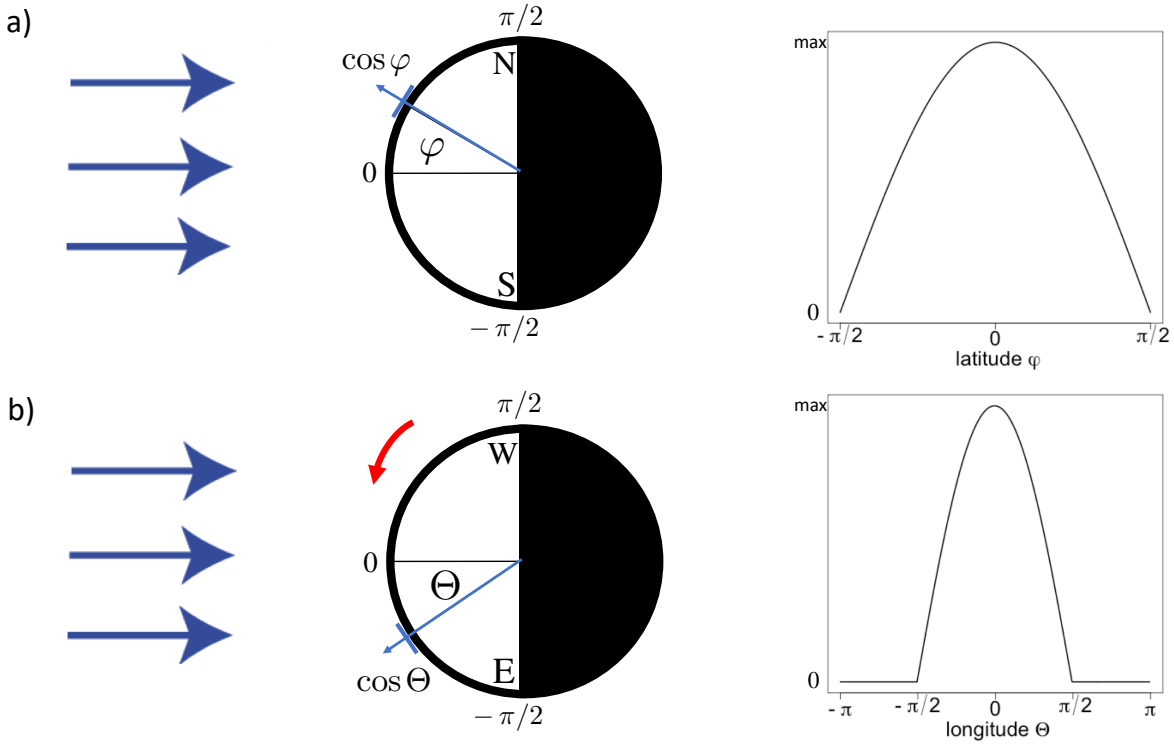


**Figure 1.** New Figure 2 in the paper: Latitudinal (a) and longitudinal (b) dependence of the incoming short wave radiation. On the right hand side, the insolation as a function of latitude $\varphi$ and longitude $\Theta$ with maximum insolation $(1-\alpha)S$ is shown. See text for the details.

we can define the angle $\Theta$ anti-clockwise on the for the sun-shining side between $-\pi/2$ and $\pi/2$. We define the maximal insolation always at $\Theta = 0$ which is moving in time. In the panel, the Earth's rotation is schematically sketched as the red arrow, and we see the time-dependence in the right-hand side. It is noted that the geographical longitude can be calculated by $mod(\Theta - 2\pi \cdot t/24, 2\pi)$ where t is measured in hours and mod is the modulo operation. Summarizing our geometrical considerations, we can now write the local energy balance as

$$\epsilon\sigma T^4 = (1-\alpha)S \cdot \cos\varphi \cdot \cos\Theta \qquad \text{for } -\pi/2 < \Theta < \pi/2 \tag{1}$$

and zero during night for $\Theta < -\pi/2$ or $\Theta > \pi/2$. Temperatures based on the local energy balance without a heat capacity would vary between $T_{min} = 0$ K and $T_{max} = \sqrt[4]{\frac{(1-\alpha)S}{\epsilon\sigma}} = \sqrt{2} \cdot \sqrt[4]{\frac{(1-\alpha)S}{4\epsilon\sigma}} = \sqrt{2} \cdot 288K = 407$ K.

Integration of (1) over the Earth surface is

$$\int_{-\pi/2}^{\pi/2}\left(\int_0^{2\pi}\epsilon\sigma T^4\, R\cos\varphi d\Theta\right)Rd\varphi = (1-\alpha)S\int_{-\pi/2}^{\pi/2}R\cos^2\varphi d\varphi\cdot\int_{-\pi/2}^{\pi/2}R\cos\Theta d\Theta$$

$$\epsilon\sigma R^2\frac{4\pi}{4\pi}\int_{-\pi/2}^{\pi/2}\left(\int_0^{2\pi}T^4\cos\varphi d\Theta\right)d\varphi = (1-\alpha)SR^2\underbrace{\int_{-\pi/2}^{\pi/2}\cos^2\varphi\, d\varphi}_{\frac{\pi}{2}}\cdot\underbrace{\int_{-\pi/2}^{\pi/2}\cos\Theta\, d\Theta}_{2}$$

$$\epsilon\sigma 4\pi\overline{T^4} = (1-\alpha)S\,\pi \tag{2}$$

giving a similar formula as (3, in the paper) with the definition for the average $\overline{T^4}$.

What we really want is the mean of the temperature $\overline{T}$. Therefore, we take the fourth root of (1):

$$T = \sqrt[4]{\frac{(1-\alpha)S\cos\varphi\cos\Theta}{\epsilon\sigma}} \qquad \text{for } -\pi/2<\Theta<\pi/2 \tag{3}$$

and zero elsewhere. If we calculate the zonal mean of (3) by integration at the latitudinal cycles we have

$$T(\varphi) = \frac{1}{2\pi}\int_{-\pi/2}^{-\pi/2}\sqrt[4]{\frac{(1-\alpha)S\cos\varphi\cos\Theta}{\epsilon\sigma}}d\Theta$$

$$= \frac{\sqrt{2}}{2\pi}\underbrace{\int_{-\pi/2}^{\pi/2}(\cos\Theta)^{1/4}d\Theta}_{\sqrt{\pi}\Gamma(5/8)/\Gamma(9/8)}\sqrt[4]{\frac{(1-\alpha)S}{4\epsilon\sigma}}\;(\cos\varphi)^{1/4} = \underbrace{\frac{1}{\sqrt{2\pi}}\frac{\Gamma(5/8)}{\Gamma(9/8)}}_{\approx 0.608}\cdot\sqrt[4]{\frac{(1-\alpha)S}{4\epsilon\sigma}}\;(\cos\varphi)^{1/4} \tag{4}$$

as a function on latitude (Fig. 3 in the paper). $\Gamma$ is Euler's Gamma function with $\Gamma(x+1)=x\Gamma(x)$. When we integrate this over the latitudes, we obtain

$$\overline{T} = \frac{1}{2}\int_{-\pi/2}^{\pi/2}T(\varphi)\cos\varphi\, d\varphi = \frac{1}{2}\frac{\Gamma(5/8)}{\sqrt{2\pi}\Gamma(9/8)}\cdot\sqrt[4]{\frac{(1-\alpha)S}{4\epsilon\sigma}}\underbrace{\int_{-\pi/2}^{\pi/2}(\cos\varphi)^{5/4}d\varphi}_{\sqrt{\pi}\Gamma(9/8)/\Gamma(13/8)}$$

$$= \frac{1}{2}\frac{1}{\sqrt{2}}\frac{\Gamma(5/8)}{\Gamma(13/8)}\cdot\sqrt[4]{\frac{(1-\alpha)S}{4\epsilon\sigma}} = \underbrace{\frac{\sqrt{2}}{4}\frac{8}{5}}_{0.4\sqrt{2}\approx 0.566}\cdot\sqrt[4]{\frac{(1-\alpha)S}{4\epsilon\sigma}} \tag{5}$$

Therefore, the mean temperature is a factor $0.4\sqrt{2}\approx 0.566$ lower than 288 K as stated at (**??**) and would be $\overline{T}=163$ K. The standard EBM in Fig. 1 (in the paper) has imprinted into our thoughts and lectures. We should therefore be careful and pinpoint the reasons for the failure. What happens here is that the heat capacity of the Earth is neglected and there is a strong non-linearity of the outgoing radiation.

**Comment 1b)**

I find it very puzzling that the heat capacity $C_p$ does not explicitly appear in eq. (11), although I clearly see how you get there. A few words of explanation would be very useful to the (less-expert) reader.

**Answer/Action**

Indeed, the equilibrium solution is calculated from (10) as there is no time-dependence due to the integration over longitude and day. In the revised version, I was better to avoid the notation of the $1_{[-\pi/2<\Theta<\pi/2]}(\Theta)$ function. The formulation is now

$$\begin{aligned} C_p\,\partial_t T &= (1-\alpha)S\cdot\cos\varphi\cdot\cos\Theta - \epsilon\sigma T^4 \qquad \text{for } -\pi/2<\Theta<\pi/2 \\ &= -\epsilon\sigma T^4 \qquad \text{elesewhere} \end{aligned}$$

Now, it becomes clear that the equilibrium solution is given. I write explicitly in line 20-21 of page 4, and line 1 on page 5 how the averaging is done.

**Comment 1c)**

Then, after eq. (12) the reference heat capacity is chosen as the atmospheric heat capacity. Why is that? Above in the text you have said that the heat capacity is manly given by the ocean, so why do you use the atmospheric heat capacity here?

**Answer/Action**

Yes, the effective heat capacity is time-scale dependent. For the day and night cycle values in the order of the atmospheric heat capacity are realistic for our Earth with 24 h rotation. In the revised version, I am more explicit here and show how the temperature would change in a slowly rotating planet (new Fig. 5).

In the section 5; I have added a discussion of the effective heat capacity. For the diurnal cycle $h_T$ is less that half a meter and the heat capacity generally less than that of the atmosphere. The seasonal mixed layer depth can be several hundred meters (e.g., de Boyer Montégut et al., 2004). As pointed out by Schwartz (2007), the effective heat capacity that reflects only that portion of the global heat capacity that is coupled to the perturbation on the timescale of the perturbation. In the context of global climate change induced by changes in atmospheric composition on the decade to century timescale the effective heat capacity is subject to change in heat content on such timescales. For the seasonal cycle and longer time scales, this issue is more difficult. I tried to avoid realistic scenarios, because than one would have to define geographical details. There is no demand for realism here.

**Comment 1d)**

A bit more explanation and motivation should also enter the fact that in one case in Fig. 5 you use a latitudinal dependent heat capacity (in the text just after eq. (12)). How exactly? And what is the motivation for that?

**Answer/Action**

Yes, this can be better motivated. The high latitudes have a much higher effective heat capacity due to the deeper mixed layer at high latitudes. It is just an assumption, see above.

**Comment 1e)**

On page 6, line 18, the temperatures T1 and T2 remain unexplained!

**Answer/Action**

In the revised version, these temperatures are better explained. It is a back-on-the-envelope calculation to see the main argument. I replaced this section by

Fig. 8 shows the seasonal amplitude for the $C_p$-scenarios as indicated by the blue and dashed black lines, respectively. ~~A change in the seasonal /diurnal cycle of $T_1 - T_2 = 50°C$ is equivalent to about $10 Wm^{-2}$ when applying the long wave radiation change $\epsilon\sigma \cdot 0.5(T_1^4 + T_2^4) - \epsilon\sigma \cdot (0.5 \cdot (T_1 + T_2))^4$ for typical temperatures on the Earth. Please note that the number $10 Wm^{-2}$ is equivalent to a greenhouse gas forcing of more than quadrupling the $CO_2$ concentration in the atmosphere.~~

~~Energy balance models have been used to diagose the temperatures on the Earth when applying complex circulation models (e.g., Knorr et al. 2011)or data (e.g., Köhler et al., 2010; van der Heydt et al., 2016; Stap~~ The larger the seasonal contrast, the colder is the climate. Let us define here $\overline{\cdot}$ as the averaging over a time period (here the seasonal cycle), then $\overline{T^4} > \overline{T}^4$ which is consistent with Hölder's inequality (Rodgers, 1888; Hölder 1889; Hardy et al., ~~2018). For the past, a strong warming at high latitudes is reconstructed for the Pliocene, Miocene, Eocene periods (Markwick, 1994; Wolfe, 1994; Sloan and Rea, 1996; Huber et al. , 2000; Shellito et al. , 2003; Tripati et al. , 2003; Mosbrugger et al., 2005; Utescher and Mosbrugger, 2007).~~ 1934, Kuptsov, 2001). It is noted that this feature is missing in the linearized version $A + B \cdot T'$ of the outgoing radiation. We see the large variation in the seasonal cycle $\Delta T = T_{summer} - T_{winter}$ for the blue line in Fig. **??** as compared to the dashed line. A mean change in the net long wave radiation can be approximated by the mean of summer and winter values $\epsilon\sigma \cdot 0.5(T_{summer}^4 + T_{winter}^4)$, which is up to $10 Wm^{-2}$ higher than $\epsilon\sigma \cdot (0.5 \cdot (T_{summer} + T_{winter}))^4$ if the seasonal cycle is damped as in the dashed line of Fig. **??**. This implies that a lower seasonal cycle provides for a significant warming. If we would consider a linear model $A + B \cdot T'$ with $T'$ being measured in $°C$ for the long-wave radiation, the differences between the blue and the dashed line would be much lower, due to the absence of the non-linearity in net long wave radiation change.

**Comment 2)**

The second point relates to the vertical mixing in the ocean. It is interesting to see how the vertical mixing in the ocean obviously can affect the equator-to-pole surface temperature gradient. However, why should the vertical mixing be so different in the Palaeogene/Neogene before 3 Ma? Tidal dissipation can play a role, but also bathymetry and probably also the number and specific geometry of the ocean gateways. But so far, this remains very speculative and unmotivated in the manuscript. For example, how does the factor 25 in the vertical mixing coefficient that is used in the GCM simulations relate to expected changes in vertical mixing due to tides and bathymetry?

**Answer/Action**

The manuscript is admittedly a little vague at this point. A more explicit statement about a more explicit calculation of the vertical mixing is beyond the scope of the present paper. I will add more literature dealing with bathymetry, tides and geometry

of the ocean in the revised version. stressed out that The effective heat capacity is not an intrinsic property of the climate system but is reflective of the rate of penetration of heat energy into the ocean in response to the particular pattern of forcing and the background state (Schwartz, 2007). I mentioned the relevance for climate warming scenarios.

However, I have boiled down this chapter, rewrote most of it, and shortened it considerably. The factor of 25 is arbritary. I wrote

In order to mimick the effect of a higher effective heat capacity and deepened mixed layer depth, the vertical mixing coefficient is increased in the ocean, changing the values for the background vertical diffusivity (arbritarily) by a factor of 25, providing a deeper thermocline.

and later

Furthermore, the model indicates that the respective winter signal of high-latitude warming is most pronounced (Fig. 9), decreasing the seasonality, suggesting a common signal of pronounced warming and weaker seasonality, a feature already seen in our EBM (Fig. 8).

and

Inspired by the EBM and GCM results, we may think of a climate system having a higher effective heat capacity producing a reduced seasonal cycle and flat temperature gradients. The changed vertical mixing coefficients are mimicking possible effects like weak tidal dissipation or abyssal stratification (e.g., Lambeck 1977; Green and Huber, 2013), but its explicit physics is not evaluated here.

Therefore, I deleted some text which was formally in there, given several arguments for expected changes in vertical mixing due to tides and bathymetry.

# Answer to interactive comment of referee #2 on "Temperatures from Energy Balance Models: the effective heat capacity matters"

Gerrit Lohmann[1,2]

[1]Alfred Wegener Institute, Helmholtz Centre for Polar and Marine Research, Bremerhaven, Germany
[2] University of Bremen, Bremen, Germany

Thanks for the detailed critics on the *Interactive comment on Earth Syst. Dynam. Discuss., https://doi.org/10.5194/esd-2019-35, 2019.* by referee #2. The comments were helpful in improving the readability of the manuscript. In the following, I repeat and answer to these comments. Furthermore, the actions are described.

**Comment 1**

Eq. (4)

$$\epsilon\sigma T^4(\Theta,\varphi) \quad = \quad (1-\alpha)S \quad \cos\varphi \quad \cos\Theta \quad \times \quad 1_{[-\pi/2<\Theta<\pi/2]}(\Theta)$$

is not a good description of the energy balance on the surface of the earth. A description of the spatial distribution of energy requires an introduction of energy redistribution by ocean currents, eddies, etc. Further, sun?s declination angle should be taken into account in order to describe reasonable spatial distribution of energy at any specific time of the year. What is described here is, at best, an energy balance in an annual-mean sense when there is no physical mechanism for redistribution of strong energy surplus in the equatorial region and strong energy deficit in the polar region.

**Answer/Action**

The left-hand side of (4) as well as the right-hand side are latitude $\varphi$- and longitute $\Theta$-dependent. The incoming radiation goes with the cosine of latitude and longitude, and there is only sunshine during the day. This is noted as the $1_{[-\pi/2<\Theta<\pi/2]}(\Theta)$ function which is zero outside the interval $[-\pi/2 < \Theta < \pi/2]$. The global mean temperature is not affected by the obliquity and precession (Berger and Loutre 1991; 1997; Laepple and Lohmann 2009). Therefore, we ignore the Earth orbital parameters for a while which makes an analytical calculation possible. Later in the numerical treatment, the full seasonal cycle is taken into account (former equation (16) in the manuscript). Indeed, eq. (4) is now better explained and motivated.

I have rewritten section 2, added a figure, and I think the notation is now clearer.

The incoming radiation goes with the cosine of latitude $\varphi$ and longitude $\Theta$, and there is only sunshine during the day. Fig. 1a shows the latitudinal dependence. As we assume no tilt (this assumption is later relaxed), the latitudinal dependence is a function of latitude only: $\cos\varphi$. On the right-hand side, the function is shown. Fig. 1b shows the latitudinal dependence is a function of longitude: $\cos\Theta$ for the sun-shining side of the Earth, and for the dark side of the Earth it is zero. For simplicity, we can define the angle $\Theta$ anti-clockwise on the for the sun-shining side between $-\pi/2$ and $\pi/2$. We define the maximal

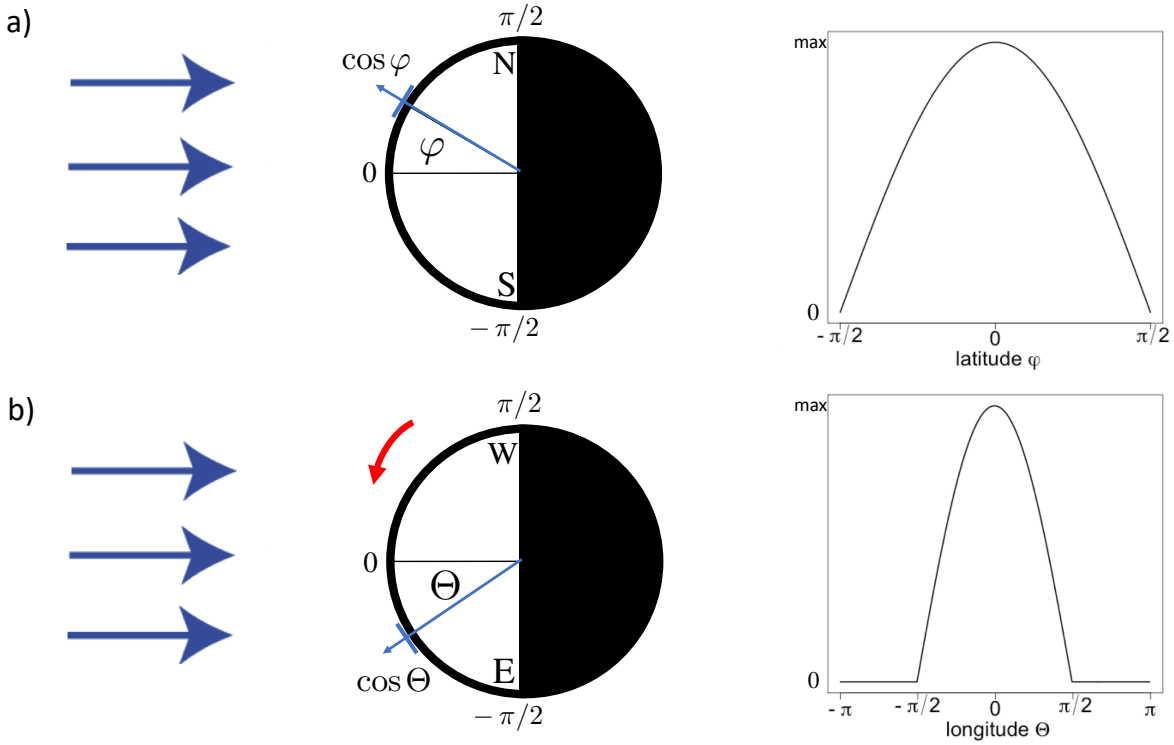


**Figure 1.** New Figure 2 in the paper: Latitudinal (a) and longitudinal (b) dependence of the incoming short wave radiation. On the right hand side, the insolation as a function of latitude $\varphi$ and longitude $\Theta$ with maximum insolation $(1-\alpha)S$ is shown. See text for the details.

insolation always at $\Theta = 0$ which is moving in time. In the panel, the Earth's rotation is schematically sketched as the red arrow, and we see the time-dependence in the right-hand side. It is noted that the geographical longitude can be calculated by $mod(\Theta - 2\pi \cdot t/24, 2\pi)$ where t is measured in hours and mod is the modulo operation. Summarizing our geometrical considerations, we can now write the local energy balance as

$$\epsilon\sigma T^4 = (1-\alpha)S \cdot \cos\varphi \cdot \cos\Theta \qquad \text{for } -\pi/2 < \Theta < \pi/2 \tag{1}$$

and zero during night for $\Theta < -\pi/2$ or $\Theta > \pi/2$. Temperatures based on the local energy balance without a heat capacity would vary between $T_{min} = 0$ K and $T_{max} = \sqrt[4]{\frac{(1-\alpha)S}{\epsilon\sigma}} = \sqrt{2} \cdot \sqrt[4]{\frac{(1-\alpha)S}{4\epsilon\sigma}} = \sqrt{2} \cdot 288K = 407$ K.

Integration of (1) over the Earth surface is

$$\int_{-\pi/2}^{\pi/2}\left(\int_0^{2\pi}\epsilon\sigma T^4\, R\cos\varphi d\Theta\right)Rd\varphi = (1-\alpha)S\int_{-\pi/2}^{\pi/2}R\cos^2\varphi d\varphi\cdot\int_{-\pi/2}^{\pi/2}R\cos\Theta d\Theta$$

$$\epsilon\sigma R^2\frac{4\pi}{4\pi}\int_{-\pi/2}^{\pi/2}\left(\int_0^{2\pi}T^4\cos\varphi d\Theta\right)d\varphi = (1-\alpha)SR^2\underbrace{\int_{-\pi/2}^{\pi/2}\cos^2\varphi\, d\varphi}_{\frac{\pi}{2}}\cdot\underbrace{\int_{-\pi/2}^{\pi/2}\cos\Theta\, d\Theta}_{2}$$

$$\epsilon\sigma 4\pi\overline{T^4} = (1-\alpha)S\,\pi \tag{2}$$

giving a similar formula as (3, in the paper) with the definition for the average $\overline{T^4}$.

What we really want is the mean of the temperature $\overline{T}$. Therefore, we take the fourth root of (1):

$$T = \sqrt[4]{\frac{(1-\alpha)S\cos\varphi\cos\Theta}{\epsilon\sigma}} \qquad \text{for } -\pi/2<\Theta<\pi/2 \tag{3}$$

and zero elsewhere. If we calculate the zonal mean of (3) by integration at the latitudinal cycles we have

$$T(\varphi) = \frac{1}{2\pi}\int_{-\pi/2}^{-\pi/2}\sqrt[4]{\frac{(1-\alpha)S\cos\varphi\cos\Theta}{\epsilon\sigma}}d\Theta$$

$$= \frac{\sqrt{2}}{2\pi}\underbrace{\int_{-\pi/2}^{\pi/2}(\cos\Theta)^{1/4}d\Theta}_{\sqrt{\pi}\Gamma(5/8)/\Gamma(9/8)}\sqrt[4]{\frac{(1-\alpha)S}{4\epsilon\sigma}}\;(\cos\varphi)^{1/4} = \underbrace{\frac{1}{\sqrt{2\pi}}\frac{\Gamma(5/8)}{\Gamma(9/8)}}_{\approx 0.608}\cdot\sqrt[4]{\frac{(1-\alpha)S}{4\epsilon\sigma}}\;(\cos\varphi)^{1/4} \tag{4}$$

as a function on latitude (Fig. 3 in the paper). $\Gamma$ is Euler's Gamma function with $\Gamma(x+1)=x\Gamma(x)$. When we integrate this over the latitudes, we obtain

$$\overline{T} = \frac{1}{2}\int_{-\pi/2}^{\pi/2}T(\varphi)\cos\varphi\, d\varphi = \frac{1}{2}\frac{\Gamma(5/8)}{\sqrt{2\pi}\Gamma(9/8)}\cdot\sqrt[4]{\frac{(1-\alpha)S}{4\epsilon\sigma}}\underbrace{\int_{-\pi/2}^{\pi/2}(\cos\varphi)^{5/4}d\varphi}_{\sqrt{\pi}\Gamma(9/8)/\Gamma(13/8)}$$

$$= \frac{1}{2}\frac{1}{\sqrt{2}}\frac{\Gamma(5/8)}{\Gamma(13/8)}\cdot\sqrt[4]{\frac{(1-\alpha)S}{4\epsilon\sigma}} = \underbrace{\frac{\sqrt{2}}{4}\frac{8}{5}}_{0.4\sqrt{2}\approx 0.566}\cdot\sqrt[4]{\frac{(1-\alpha)S}{4\epsilon\sigma}} \tag{5}$$

Therefore, the mean temperature is a factor $0.4\sqrt{2}\approx 0.566$ lower than 288 K as stated at (**??**) and would be $\overline{T}=163$ K. The standard EBM in Fig. 1 (in the paper) has imprinted into our thoughts and lectures. We should therefore be careful and pinpoint the reasons for the failure. What happens here is that the heat capacity of the Earth is neglected and there is a strong non-linearity of the outgoing radiation.

**Comment 2**

Eq. (8): This is a strange derivation. Let us consider outgoing longwave radiation and incoming solar radiation in the form

$$\epsilon\sigma T^4(\phi,\Theta) \quad = \quad (1-\alpha)S \quad \cos\phi \quad \cos\Theta \quad \times \quad 1_{[-\pi/2<\Theta<\pi/2]}(\phi)$$

where $\phi$ is longitute and $\Theta$ is latitude. Equation (1) defines energy per unit time per unit area as the dimension of $\sigma = 5.670373 \times 10^{-8} W m^{-2} K^{-4}$ indicates. Thus, total incoming radiation can be written as ...

$$(1-\alpha)S\,\pi\,R^2$$

Similarly, total outgoing radiation can be written as ...

$$\epsilon\sigma\overline{T}^4\,4\pi\,R^2$$

Thus, we arrive at

$$\overline{T} = \sqrt[4]{\frac{(1-\alpha)S}{4\epsilon\sigma}}$$

**Answer/Action**

Your equation above (in your review eq. (1)), is basically the same as the one I used. The difference is that you defined $\phi$ as longitude and $\Theta$ as latitude, whereas I do it in the other way round. (By the way: This is the same approach you criticized in your comment #1.)

The calculation you presented is also more or less the same as mine, with one **fundamental** difference. In my derivation by integration over the Earth surface

$$\epsilon\sigma 4\pi\overline{T^4} = (1-\alpha)S\,\pi\ .$$

In this formula, the average $\overline{T^4}$ is calculated, not $\overline{T}^4$. Therefore,

$$\overline{T} = \sqrt[4]{\frac{(1-\alpha)S}{4\epsilon\sigma}}$$

is not correct. This argument to exchange the $\overline{T^4}$ by $\overline{T}^4$ was one of the motivation to write down the global energy balance in a correct form. In order to $\overline{T}$, one has a more lengthy calculation: If we now calculate the zonal mean of the temperature by

integration at the latitudinal cycles we have

$$
\begin{aligned}
T(\varphi) &= \frac{1}{2\pi}\int_{-\pi/2}^{-\pi/2}\sqrt[4]{\frac{(1-\alpha)S\cos\varphi\cos\Theta}{\epsilon\sigma}}d\Theta \\
&= \frac{\sqrt{2}}{2\pi}\underbrace{\int_{-\pi/2}^{\pi/2}(\cos\Theta)^{1/4}d\Theta}_{=\sqrt{\pi}\Gamma(5/8)/\Gamma(9/8)}\quad\sqrt[4]{\frac{(1-\alpha)S}{4\epsilon\sigma}}\quad(\cos\varphi)^{1/4} \\
&= \frac{1}{\sqrt{2\pi}}\frac{\Gamma(5/8)}{\Gamma(9/8)}\cdot\sqrt[4]{\frac{(1-\alpha)S}{4\epsilon\sigma}}\quad(\cos\varphi)^{1/4} \\
&= 0.608\cdot\sqrt[4]{\frac{(1-\alpha)S}{4\epsilon\sigma}}\quad(\cos\varphi)^{1/4}
\end{aligned}
$$

as a function of latitude. $\Gamma$ is Euler's Gamma function with $\Gamma(x+1)=x\Gamma(x)$. When we integrate this over the latitudes, we obtain

$$
\begin{aligned}
\overline{T} &= \frac{1}{2}\int_{-\pi/2}^{\pi/2}T(\varphi)\cos\varphi\,d\varphi \\
&= \frac{1}{2}\frac{\Gamma(5/8)}{\sqrt{2\pi}\Gamma(9/8)}\cdot\sqrt[4]{\frac{(1-\alpha)S}{4\epsilon\sigma}}\quad\underbrace{\int_{-\pi/2}^{\pi/2}(\cos\varphi)^{5/4}d\varphi}_{=\sqrt{\pi}\Gamma(9/8)/\Gamma(13/8)} \\
&= \frac{1}{2}\frac{1}{\sqrt{2}}\frac{\Gamma(5/8)}{\Gamma(13/8)}\sqrt[4]{\frac{(1-\alpha)S}{4\epsilon\sigma}} = \frac{\sqrt{2}}{4}\frac{8}{5}\sqrt[4]{\frac{(1-\alpha)S}{4\epsilon\sigma}} \\
&= 0.4\sqrt{2}\sqrt[4]{\frac{(1-\alpha)S}{4\epsilon\sigma}} = 0.566\sqrt[4]{\frac{(1-\alpha)S}{4\epsilon\sigma}}
\end{aligned}
$$

As a side remark: The fact that $\sqrt[4]{\overline{T^4}}$ is higher than $\overline{T}$ is consistent with Hölder's inequality (Rodgers, 1888; Hölder 1889; Hardy et al., 1934, Kuptsov, 2001). This now mentioned in the revised version of the manuscript.

**Comment 3**

Specific heat is not needed to reproduce the reasonable spatial distribution of temperature. For example, 1D energy balance model with meridional heat flux can be written as (see North and Kim, 2017; p123-134)

$$-\frac{d}{d\mu}\left(D(1-\mu^2)\frac{dT(\mu)}{d\mu}\right)+A+BT(\mu,t)=Qa(\mu)s(\mu)$$

...

with a realistic insolation distribution function and a realistic albedo (see North and Kim, 2017 for details), we obtain a solution as in Figure 1. The model solution is fairly similar to the observational data. Further, the diffusive heat transport in a zonal mean sense looks very reasonable compared to that derived from satellite observations (see Figure 2).

**Answer/Action**

Thanks for your comment and hinting to the important work of North and Kim (2017). As I mention in the manuscript: "The linearization of the long wave radiation in several models (North et al., 1975a, b; Chen et al., 1995) implicitly assumes the above heat capacity and fast rotation arguments. " Indeed, the linearized version can give a reasonable zonal mean climate.

In the revised version, I stress out this more clearly. My point is that we need a rapidly rotating object with significant heat capacity. Without these effects, the global mean temperature would be lower.

I inserted the text: Quite often the linearization the long wave radiation $\epsilon\sigma T^4$ is linearized in energy balance models. Indeed the linearization is performed around $0°C$ (North et al., 1975a, b; Chen et al., 1995; Lohmann and Gerdes, 1998; North and Kim, 2017) and is formulated as $A + B \cdot T'$ with $T'$ being measured in $°C$. As the temperatures based on the local energy balance without a heat capacity would vary between $T_{min} = 0$ K and $T_{max} = \sqrt{2} \cdot 288K = 407$ K, a linearization would be not permitted. Therefore, the linearization implicitely assumes the above heat capacity and fast rotation arguments.

I show that other processes - like horizontal transport processes - are only of secondary importance for the globally averaged temperature (Figs. 3 and 6) The finding is furthermore important to see that the effective heat capacity (which is time-scale dependent) has a direct influence on the global (and regional) temperatures (Figs. 4 and 5). Fig. 5 shows how the temperature would change in a slowly rotating planet.

**Comment 4**

"The atmospheric circulation provides an efficient way to propagate heat along latitudes which is ignored and is a second order effect (not shown)." This statement is erroneous. As demonstrated in Comment #3 above, a reasonable temperature distribution on the surface of the earth is reproduced by using diffusive heat transport. Heat capacity is not even used in this calculation of equilibrium temperature.

**Answer/Action**

Yes, this can be better motivated. Indeed, the energy input is time-dependent. Therefore, the mean and latitudinal temperature depends on the time derivative. See also my comments and action points in answer to Comment #3. As seen in the manuscript, the temperatures do depend on the effective heat capacity.

In the revised version, I am clearer is stating in the abstract

Energy balance models (EBM) are highly simplified systems of the climate system. The global temperature is calculated by the radiation budget through the incoming energy from the Sun and the outgoing energy from the Earth. The argument that the temperature can be calculated by the simple radiation budget is revisited. The underlying assumption for a realistic temperature distribution is explored: One has to assume a moderate diurnal cycle due to the large heat capacity and the fast rotation of the Earth. Interestingly, the global mean in the revised EBM is very close to the originally proposed value.

**Comment 5**

Eq. (12): The author introduced diurnal cycle of temperature and determined the global average of the averaged diurnal cycle of temperature. This discussion is erroneous. We can write diurnal temperature change as ...

Further, incoming solar radiation has the same form as in (1). Thus, we arrive at the same conclusion as in Comment #2.

**Answer/Action**

Thanks for making this hint. Indeed, I agree to your basic equation (1), but not with the conclusion. See my answer to your Comment #2.

**Comment 6**

A time-dependent 1D EBM can be written as ...

Equation (12) is equivalent to (6) as far as the annual mean temperature is concerned. Obviously, an adequate explanation is needed in terms of how Figure 3 is produced.

**Answer/Action**

I agree for the linearized EBM. See my answer to your Comment #3. I explicitly state that in the linearized EBM, the heat capacity argument is implicitly included. in the abstract: A linearized EBM implicitly assumes the heat capacity and the fast rotation arguments.

and

Quite often the linearization the long wave radiation $\epsilon\sigma T^4$ is linearized in energy balance models. Indeed the linearization is performed around $0°C$ (North et al., 1975a, b; Chen et al., 1995; Lohmann and Gerdes, 1998; North and Kim, 2017) and is formulated as $A + B \cdot T'$ with $T'$ being measured in $°C$. As the temperatures based on the local energy balance without a heat capacity would vary between $T_{min} = 0$ K and $T_{max} = \sqrt{2} \cdot 288K = 407$ K, a linearization would be not permitted. Therefore, the linearization implicitely assumes the above heat capacity and fast rotation arguments.

Furthermore, parameter study of Figure 3 is better explained. The model that I use is the non-linear model with the $T^4$-term and a time-dependent forcing. I insert furthermore Fig. 4 with the temperature dependence on heat capacity (and rotation rate) when analyzing the diurnal cycle.

**Comment 7**

Figure 3: The main effect of heat capacity in the original EBM is in the context of the amplitude of the annual and semi-annual cycles (see North and Kim, p152). The annual and semi-annual cycles are seriously affected by the choice of heat capacity, whereas the annual mean component is not. The author should demonstrate that not only annual-mean temperature distribution but also the annual and semi-annual cycles of temperature is reproduced reasonably by their choice of heat capacity (see, for example, Fig. 6.8 of North and Kim).

**Answer/Action**

Thanks again for your comment and for hinting at the important work of North and Kim (2017). Yes, I agree for the linearized EBM. See my answer to your Comment #3 and #6. In the non-linear model, the temperature is affected by the heat capacity. The effective heat capacity is important as it is reflective of the rate of penetration of heat energy into the ocean in response to the particular pattern of forcing and the background state (Schwartz, 2007). I also emphasize the relevance of this for climate scenarios.

In section 5, I write now For the diurnal cycle $h_T$ is less that half a meter and the heat capacity generally less than that of the atmosphere. The seasonal mixed layer depth can be several hundred meters (e.g., de Boyer Montégut et al., 2004). As pointed out by Schwartz (2007), the effective heat capacity that reflects only that portion of the global heat capacity that is coupled to the perturbation on the timescale of the perturbation. In the context of global climate change induced by changes in atmospheric composition on the decade to century timescale the effective heat capacity is subject to change in heat content on such timescales.

I explicitly show the results of the linearized EBM here. In principle there is no principle difference to the non-linear model, although in detail the distribution is different.

In section 4, I now explicitly write Fig. 8 shows the seasonal amplitude for the $C_p$-scenarios as indicated by the blue and dashed black lines, respectively. The larger the seasonal contrast, the colder is the climate. Let us define here $\bar{\cdot}$ as the averaging over a time period (here the seasonal cycle), then $\overline{T^4} > \overline{T}^4$ which is consistent with Hölder's inequality (Rodgers, 1888; Hölder 1889; Hardy et al., 1934, Kuptsov, 2001). It is noted that this feature is missing in the linearized version $A + B \cdot T'$ of the outgoing radiation. We see the large variation in the seasonal cycle $\Delta T = T_{summer} - T_{winter}$ for the blue line in Fig. **??** as compared to the dashed line. A mean change in the net long wave radiation can be approximated by the mean of summer and winter values $\epsilon\sigma \cdot 0.5(T^4_{summer} + T^4_{winter})$, which is up to $10\,Wm^{-2}$ higher than $\epsilon\sigma \cdot (0.5 \cdot (T_{summer} + T_{winter}))^4$ if the seasonal cycle is damped as in the dashed line of Fig. 8. This implies that a lower seasonal cycle provides for a significant warming. If we would consider a linear model $A + B \cdot T'$ with $T'$ being measured in $^\circ C$ for the long-wave radiation, the differences between the blue and the dashed line would be much lower, due to the absence of the non-linearity in net long wave radiation change.

This clarifies the difference between a linear and non-linear model.

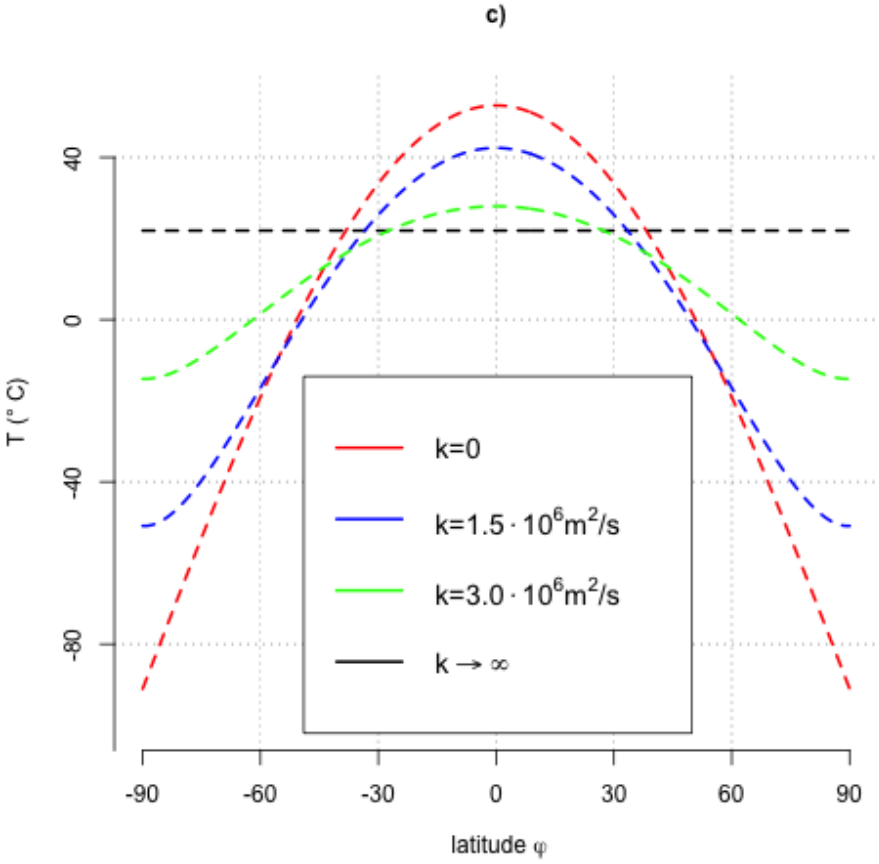


**Figure 2.** Equilibrium temperature of the linearized EBM using different diffusion coefficients. ). Units are °C.

**Comment 8**

P8 L20: What does the first law of thermodynamics have anything to do with incoming radiation = outgoing radiation? Is the author referring to the zeroth law of thermodynamics?

**Answer/Action**

Thanks. This is indeed not well formulated. In the revised version, I deleted the phrase $1^{st}$ law of thermodynamics on the

**Comment 9**

As already demonstrated in Comment #2, global average temperature is close to the observed value without the effect of heat capacity. Further, by using diffusive heat transport, zonally average temperature is reproduced close to actual observation in Comment #3.

**Answer/Action**

Thanks. I disagree and point to my answers to Comments #2 and #3.

**Comment 10**

It is difficult to review the entire manuscript until my earlier comments are fully addressed. In particular, the author needs to explain clearly how the solutions in each figure are computed (with appropriate equation if possible) and demonstrate clearly that his full solution (with diurnal and annual cycles) matches reasonably with the observations for his choice of heat capacity.

**Answer/Action**

I agree that it seems a misunderstanding. My answers to Comments #2 and #3 shall clarify the mistake in the calculation of the temperature. The time dependence is more explicitly stated. Furthermore, the non-linearity in the outgoing radiation makes this model different from your EBMs. The equations for the EBMs used are in the manuscript. For the equations, it is important to explicitly spell out the assumptions made. See my answer to your Comments #3 and #6. It is now explicitly stated that in the linearized EBM, the heat capacity argument is implicitly included. The model that I use is the non-linear model with the $T^4$-term and a time-dependent forcing.

Furthermore, I refer to the results of the linearized EBM in the revised version. Indeed, the linear model has some advantages because it directly indicated the climate sensitivity. However, for a rigorous derivation of the global and regional effects, the non-linear version is an advantage. Finally, it is necessary to see that $\overline{T^4}$ is not $\overline{T}^4$. Simplified and conceptual models can be used to study long-term climate (Hasselmann, 1976; Lemke, 1977; Timmermann and Lohmann, 2000; Lohmann, 2018). As pointed out in the manuscript, the effective heat capacity is important to understand past and potential future climate.

**Technical Comment 1**

There is, in general, lack of explanation for variables used in the equations.

**Answer/Action**

Thanks. I have gone through all equations in the manuscript to avoid misunderstandings.

**Technical Comment 2**

"shown in Fig. 2 as the (read) red line with the mean ?"

**Answer/Action**

Thanks, corrected.

# Answer to interactive comment of Referee #3 on "Temperatures from Energy Balance Models: the effective heat capacity matters"

Gerrit Lohmann[1,2]

[1]Alfred Wegener Institute, Helmholtz Centre for Polar and Marine Research, Bremerhaven, Germany
[2] University of Bremen, Bremen, Germany

Thanks for the constructive critics in the *Interactive comment on Earth Syst. Dynam. Discuss., https://doi.org/10.5194/esd-2019-35, 2019.* by referee #3. In the following, I repeat and answer to these comments. Furthermore, the actions are documented.

**Comment 1**

Neglecting the diurnal cycle in EBMs is a rather standard procedure. This assumes that the Earth receives a mean daily incoming solar energy equally distributed over each latitude bands. This is indeed most of the time quite a reasonable hypothesis for such simplified models, since the ocean surface temperature diurnal changes are small (at most a few degrees). This paper confirms this usual assumption, with the red and dotted brownish curves of Figure 2 being almost indistinguishable.

The presentation on this section is however extremely confusing. The author starts with the classical 0-dimensional time average EBM. He then presents the 1-dimensional case with a daily cycle as an extension, just introducing it as a local extension of the 0-dimensional case. However, considering that there is a local energy balance is not a valid assumption in general, contrary to the one at the global scale. Obviously, it is clearly entirely irrelevant to consider that there can be an instantaneous radiative equilibrium, with temperatures dropping to zero Kelvin as soon as the Sun sets. This is clearly not what people usually assume when using EBMs !

The usual starting point corresponds to equations (11-12) where the solar forcing is averaged over one Earth rotation. This is more or less what people have been using in geographically explicit EBMs, including the very first ones. Budyko and Sellers 1969 where indeed geographically explicit, without a diurnal cycle, as in equation (11). The authors comes back to it as a compensation of the incoherent assumption of a local radiative equilibrium. So part 2 is just showing that an irrelevant hypothesis produces irrelevant results. It brings nothing interesting, but only confusion.

To add to the confusion some assumptions are clearly not explained. On the top of page 4, the first equation is clearly invalid unless strong hypotheses are imposed, which are not specified in the text.

**Answer/Action**

The confusion shall be clarified. This manuscript revisits the relationship between the (global mean) surface temperature of the Earth and its radiation budget as is frequently used in Energy balance models (EBMs). The main point is, that the effective

heat capacity (and its temporal variation over the daily/seasonal cycle) needs to be taken into account when estimating surface temperature from the energy budget. As a starting point, a zero-dimensional model of the radiative equilibrium of the Earth is introduced

$$(1-\alpha)S\pi R^2 = 4\pi R^2 \epsilon\sigma T^4 \tag{1}$$

where the left-hand side represents the incoming energy from the Sun while the right-hand side represents the outgoing energy from the Earth. This is used to calculate the temperature

$$T = \sqrt[4]{\frac{(1-\alpha)S}{4\epsilon\sigma}} \tag{2}$$

The wording "This is clearly not what people usually assume when using EBMs " shows that there are implicit assumptions in the approach. To my point of view, the assumptions can be explicitly spelled out to obtain arguments which steps are necessary to make. I show that the global energy balance should not be calculated from this approach, because it neglects the implicit assumption of a fast rotating Earth with significant heat capacity. I am not aware of a paper which explicitly shows that

$$T = 0.989 \sqrt[4]{\frac{(1-\alpha)S}{4\epsilon\sigma}} \quad . \tag{3}$$

The author knows the fundamental work of Budyko (1969) and Sellers (1969) where the EBM could be geographically explicit, but their result has not be used to calculate the mean temperature (3).

Your statement that the author comes back to the geographically explicit EBM as a compensation of the incoherent assumption of a local radiative equilibrium cannot be found in the manuscript. The calculation of the global mean temperature from the energy balance is not irrelevant.

Your final point is that the first equation on the top of page 4 is clearly invalid unless strong hypotheses are imposed, which are not specified in the text. If you see the text above this equation, it is clearly written that it is about the diurnal variation. In a revised version, I explicitly spell out that this approximation is exactly the point of the low diurnal cycle due to the heat capacity.

I have rewritten section 2, added a figure, and I think the notation is now clearer.

The incoming radiation goes with the cosine of latitude $\varphi$ and longitude $\Theta$, and there is only sunshine during the day. Fig. 1a shows the latitudinal dependence. As we assume no tilt (this assumption is later relaxed), the latitudinal dependence is a function of latitude only: $\cos\varphi$. On the right-hand side, the function is shown. Fig. 1b shows the latitudinal dependence is a function of longitude: $\cos\Theta$ for the sun-shining side of the Earth, and for the dark side of the Earth it is zero. For simplicity, we can define the angle $\Theta$ anti-clockwise on the for the sun-shining side between $-\pi/2$ and $\pi/2$. We define the maximal insolation always at $\Theta = 0$ which is moving in time. In the panel, the Earth's rotation is schematically sketched as the red arrow, and we see the time-dependence in the right-hand side. It is noted that the geographical longitude can be calculated by $mod(\Theta - 2\pi \cdot t/24, 2\pi)$ where t is measured in hours and mod is the modulo operation. Summarizing our geometrical considerations, we can now write the local energy balance as

$$\epsilon\sigma T^4 = (1-\alpha)S \cdot \cos\varphi \cdot \cos\Theta \qquad \text{for } -\pi/2 < \Theta < \pi/2 \tag{4}$$

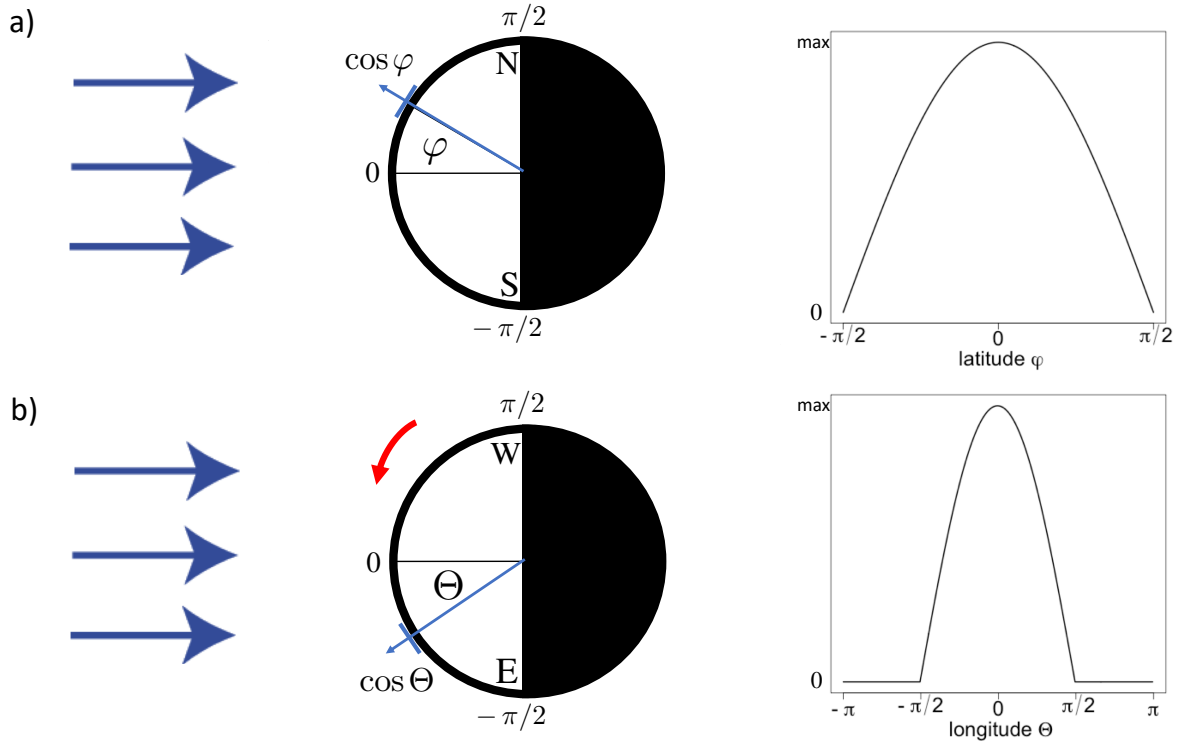


**Figure 1.** New Figure 2 in the paper: Latitudinal (a) and longitudinal (b) dependence of the incoming short wave radiation. On the right hand side, the insolation as a function of latitude $\varphi$ and longitude $\Theta$ with maximum insolation $(1-\alpha)S$ is shown. See text for the details.

and zero during night for $\Theta < -\pi/2$ or $\Theta > \pi/2$. Temperatures based on the local energy balance without a heat capacity would vary between $T_{min} = 0$ K and $T_{max} = \sqrt[4]{\frac{(1-\alpha)S}{\epsilon\sigma}} = \sqrt{2} \cdot \sqrt[4]{\frac{(1-\alpha)S}{4\epsilon\sigma}} = \sqrt{2} \cdot 288K = 407$ K.

Integration of (4) over the Earth surface is

$$\int_{-\pi/2}^{\pi/2} \left( \int_0^{2\pi} \epsilon\sigma T^4 R\cos\varphi d\Theta \right) R d\varphi = (1-\alpha)S \int_{-\pi/2}^{\pi/2} R\cos^2\varphi d\varphi \cdot \int_{-\pi/2}^{\pi/2} R\cos\Theta d\Theta$$

$$\epsilon\sigma R^2 \frac{4\pi}{4\pi} \int_{-\pi/2}^{\pi/2} \left( \int_0^{2\pi} T^4 \cos\varphi d\Theta \right) d\varphi = (1-\alpha)SR^2 \underbrace{\int_{-\pi/2}^{\pi/2} \cos^2\varphi \, d\varphi}_{\frac{\pi}{2}} \cdot \underbrace{\int_{-\pi/2}^{\pi/2} \cos\Theta \, d\Theta}_{2}$$

$$\epsilon\sigma 4\pi \overline{T^4} = (1-\alpha)S\,\pi \tag{5}$$

giving a similar formula as (3, in the paper) with the definition for the average $\overline{T^4}$.

What we really want is the mean of the temperature $\overline{T}$. Therefore, we take the fourth root of (4):

$$T = \sqrt[4]{\frac{(1-\alpha)S\cos\varphi\cos\Theta}{\epsilon\sigma}} \qquad \text{for } -\pi/2 < \Theta < \pi/2 \tag{6}$$

and zero elsewhere. If we calculate the zonal mean of (6) by integration at the latitudinal cycles we have

$$\begin{aligned} T(\varphi) &= \frac{1}{2\pi}\int_{-\pi/2}^{-\pi/2}\sqrt[4]{\frac{(1-\alpha)S\cos\varphi\cos\Theta}{\epsilon\sigma}}d\Theta \\ &= \underbrace{\frac{\sqrt{2}}{2\pi}\int_{-\pi/2}^{\pi/2}(\cos\Theta)^{1/4}d\Theta}_{\sqrt{\pi}\Gamma(5/8)/\Gamma(9/8)}\sqrt[4]{\frac{(1-\alpha)S}{4\epsilon\sigma}}\;(\cos\varphi)^{1/4} = \underbrace{\frac{1}{\sqrt{2\pi}}\frac{\Gamma(5/8)}{\Gamma(9/8)}}_{\approx 0.608}\cdot\sqrt[4]{\frac{(1-\alpha)S}{4\epsilon\sigma}}\;(\cos\varphi)^{1/4} \end{aligned} \tag{7}$$

as a function on latitude (Fig. 3 in the paper). $\Gamma$ is Euler's Gamma function with $\Gamma(x+1) = x\Gamma(x)$. When we integrate this over the latitudes, we obtain

$$\begin{aligned} \overline{T} &= \frac{1}{2}\int_{-\pi/2}^{\pi/2}T(\varphi)\cos\varphi\,d\varphi = \frac{1}{2}\frac{\Gamma(5/8)}{\sqrt{2\pi}\Gamma(9/8)}\cdot\sqrt[4]{\frac{(1-\alpha)S}{4\epsilon\sigma}}\underbrace{\int_{-\pi/2}^{\pi/2}(\cos\varphi)^{5/4}d\varphi}_{\sqrt{\pi}\Gamma(9/8)/\Gamma(13/8)} \\ &= \frac{1}{2}\frac{1}{\sqrt{2}}\frac{\Gamma(5/8)}{\Gamma(13/8)}\cdot\sqrt[4]{\frac{(1-\alpha)S}{4\epsilon\sigma}} = \underbrace{\frac{\sqrt{2}}{4}\frac{8}{5}}_{0.4\sqrt{2}\approx 0.566}\cdot\sqrt[4]{\frac{(1-\alpha)S}{4\epsilon\sigma}} \end{aligned} \tag{8}$$

Therefore, the mean temperature is a factor $0.4\sqrt{2} \approx 0.566$ lower than 288 K as stated at (2) and would be $\overline{T} = 163$ K. The standard EBM in Fig. 1 (in the paper) has imprinted into our thoughts and lectures. We should therefore be careful and pinpoint the reasons for the failure. What happens here is that the heat capacity of the Earth is neglected and there is a strong non-linearity of the outgoing radiation.

**Comment 2**

The second part of the paper discusses the role of heat capacity in the ?diurnal averaging? of temperatures. Results are summarized on Fig.3. As discussed above, the fact that temperatures are much lower for small heat capacities is rather obvious (with Earth losing most of, or all its thermal energy during the night).

**Answer/Action**

I am not aware of a study analyzing the effect of the heat capacity on global climate. Indeed, the manuscript shows this effect in Fig. 4 of the revised paper. The effective heat capacity is time-scale dependent. For the day and night cycle values in the order of the atmospheric heat capacity are realistic for our Earth with 24 h rotation. In the revised version, I am more explicit here and show how the temperature would change in a slowly rotating planet (new Fig. 5). The heat capacity plays also a role when dealing with the seasonal cycle (Figs. 7 and 8).

**Comment 3**

Using the typical oceanic vertical diffusivities for estimating a heat capacity is not very relevant. The diurnal cycle is buffered by the very top layers of the ocean that are usually almost well-mixed by winds and also by the diurnal cycle itself. The interior ocean vertical diffusivity has no role.

**Answer/Action**

The effective heat capacity is indeed time-scale dependent. In section 5, I write now For the diurnal cycle $h_T$ is less that half a meter and the heat capacity generally less than that of the atmosphere. The seasonal mixed layer depth can be several hundred meters (e.g., de Boyer Montégut et al., 2004). As pointed out by Schwartz (2007), the effective heat capacity that reflects only that portion of the global heat capacity that is coupled to the perturbation on the timescale of the perturbation. In the context of global climate change induced by changes in atmospheric composition on the decade to century timescale the effective heat capacity is subject to change in heat content on such timescales.

**Comment 4**

I do not see what is the purpose of solving equation (15) and showing Figure 4. This does not relate to the diurnal cycle, nor to heat capacity, nor to vertical mixing. What is the point ? The statement “global mean temperature is not affected by the transport because of the boundary condition. . .." is a bit strange. I would write more simply that here, global mean temperature is a measure of global heat content (uniform heat capacity) which depends only of global net radiative fluxes, not internal redistribution.

**Answer/Action**

The purpose of equation (15) and former Fig. 4 was to show the influences of the meridional heat transport and the seasonal cycle. They do not change the global mean temperature, but the temperature gradient. The statement “global mean temperature is not affected by the transport because of the boundary condition" was written to show the reader that the heat transport does not play a role (unless other feedbacks are included). In the revised version, I adopted your formulation.

**Comment 5**

Bottom of page 5 “Until now we assumed that the Earth‘s axis ...": It is quite awkward to explain only now where equation (4) page 2 comes from. Indeed equation (4) is certainly not standard for the Earth in particular in the context of EBMs and climate modeling. A planet with no tilt has no seasonal cycle. Many EBMs have an explicit seasonal cycle. Again, the starting point of the paper is very awkward.

**Answer/Action**

At the bottom of page 5, it is not the first point where equation (4) comes from. Equation (4) comes directly from the basic incoming radiation. I re-wrote the paragraph (see your comment 1). I see now the point that the motivation for equation (4) in the manuscript needs a better introduction. The beauty of (4) is that we ignore the Earth orbital parameters first (no obliquity

and no precession) which makes an analytical calculation possible. The global mean temperatures are not affected by the tilt and the values are identical to the one calculated. Indeed is stated earlier in the manuscript.

Let us have a closer look onto (1) and consider local radiative equilibrium of the Earth at each point. Fig. 1 shows the latittude-longitude dependence of the incoming short wave radiation. The global mean temperatures are not affected by the tilt (Berger and Loutre 1991; 1997; Laepple and Lohmann 2009). We assume an idealized geometry of the Earth, no obliquity and no precession, which makes an analytical calculation possible.

**Comment 6**

In the last part, the author presents some experiments with the COSMOS coupled model, to investigate the role of vertical mixing on the meridional temperature gradient. Unfortunately, it is not clear at all that these results are linked to the diurnal cycle or heat capacity. The author sets an experiment with an 25-fold increase in the background diffusivity. The logical outcome of this experiment should be to increase dramatically the oceanic circulation (not shown in the manuscript) and thus to increase massively the heat transport and the vertical mixing in the ocean. How does this relate to the heat capacity or the diurnal cycle is a mystery for me and how conclusions can be drawn from there is likewise impossible to understand. The only clear result is a weakening of the equator-to-pole gradient (likely due to increase heat transport by the ocean); however there is no physical basis to link this to past climates as the author is doing, since no probable mechanism can be suggested to increase the diffusivity by a factor 25 globally.

**Answer/Action**

Energy balance models have been used to diagose the temperatures on the Earth when applying complex circulation models. The outcome of the new approach is that effective heat capacity matters for the climate system. This cannot be seen in

$$T = \sqrt[4]{\frac{(1-\alpha)S}{4\epsilon\sigma}} \tag{9}$$

The motivation is that we may think of a climate system having a higher net heat capacity producing flat temperature gradients and reduced seasonal cycle. I replaced this section by

Fig. 8 shows the seasonal amplitude for the $C_p$-scenarios as indicated by the blue and dashed black lines, respectively. ~~A change in the seasonal /diurnal cycle of $T_1 - T_2 = 50°$C is equivalent to about $10\,Wm^{-2}$ when applying the long wave radiation change $\epsilon\sigma \cdot 0.5(T_1^4 + T_2^4) - \epsilon\sigma \cdot (0.5 \cdot (T_1 + T_2))^4$ for typical temperatures on the Earth. Please note that the number $10\,Wm^{-2}$ is equivalent to a greenhouse gas forcing of more than quadrupling the $CO_2$ concentration in the atmosphere.~~

~~Energy balance models have been used to diagose the temperatures on the Earth when applying complex circulation models (e.g., Knorr et al. 2011)or data (e.g., Köhler et al., 2010; van der Heydt et al., 2016; Stap~~ The larger the seasonal contrast, the colder is the climate. Let us define here $\bar{\cdot}$ as the averaging over a time period (here the seasonal cycle), then $\overline{T^4} > \overline{T}^4$ which is consistent with Hölder's inequality (Rodgers, 1888; Hölder 1889; Hardy et al., ~~2018). For the past, a strong warming at high latitudes is reconstructed for the Pliocene, Miocene, Eocene periods (Markwick, 1994; Wolfe, 1994; Sloan and Rea, 1996; Huber et al. , 2000; Shellito et al. , 2003; Tripati et al. , 2003; Mosbrugger et al., 2005; Utescher and Mosbrugger, 2007).~~ 1934, Kuptsov, 2001). It is noted that this feature is missing in the linearized version $A + B \cdot T'$ of the outgoing radiation.

We see the large variation in the seasonal cycle $\Delta T = T_{summer} - T_{winter}$ for the blue line in Fig. **??** as compared to the dashed line. A mean change in the net long wave radiation can be approximated by the mean of summer and winter values $\epsilon\sigma \cdot 0.5(T^4_{summer} + T^4_{winter})$, which is up to $10 Wm^{-2}$ higher than $\epsilon\sigma \cdot (0.5 \cdot (T_{summer} + T_{winter}))^4$ if the seasonal cycle is damped as in the dashed line of Fig. **??**. This implies that a lower seasonal cycle provides for a significant warming. If we would consider a linear model $A + B \cdot T'$ with $T'$ being measured in $^\circ C$ for the long-wave radiation, the differences between the blue and the dashed line would be much lower, due to the absence of the non-linearity in net long wave radiation change.

I rewrote most of the section, shortened it and elaborated the link to the seasonal cycle. The aim was to show one of the potential consequences of the effective heat capacity to explore the full range of solutions. Indeed, the increase in the mixing is admittedly ad hoc. Therefore, I have boiled down this chapter, rewrote most of it, and shortened it considerably. I wrote

In order to mimick the effect of a higher effective heat capacity and deepened mixed layer depth, the vertical mixing coefficient is increased in the ocean, changing the values for the background vertical diffusivity (arbritarily) by a factor of 25, providing a deeper thermocline.

and later

Furthermore, the model indicates that the respective winter signal of high-latitude warming is most pronounced (Fig. 9), decreasing the seasonality, suggesting a common signal of pronounced warming and weaker seasonality, a feature already seen in our EBM (Fig. 8).

and

Inspired by the EBM and GCM results, we may think of a climate system having a higher effective heat capacity producing a reduced seasonal cycle and flat temperature gradients. The changed vertical mixing coefficients are mimicking possible effects like weak tidal dissipation or abyssal stratification (e.g., Lambeck 1977; Green and Huber, 2013), but its explicit physics is not evaluated here.

**Comment 7**

In the conclusion, there are some mentions of possible linearization of the long wave radiation. Since this is critical to the whole paper (averaging T is not the same as averaging $T^4$ ), I am surprised not to see a much more detailed discussion of this point much earlier in the paper.

**Answer/Action**

In the revised version, I can stress out this more clearly. My point is that we need a rapidly rotating object with significant heat capacity. Without these effects, the global mean temperature would be lower. I explicitly state that in the linearized EBM, the heat capacity argument is implicitly included. in the abstract: A linearized EBM implicitly assumes the heat capacity and the fast rotation arguments.

and

Quite often the linearization the long wave radiation $\epsilon\sigma T^4$ is linearized in energy balance models. Indeed the linearization is

performed around $0°C$ (North et al., 1975a, b; Chen et al., 1995; Lohmann and Gerdes, 1998; North and Kim, 2017) and is formulated as $A + B \cdot T'$ with $T'$ being measured in $°C$. As the temperatures based on the local energy balance without a heat capacity would vary between $T_{min} = 0$ K and $T_{max} = \sqrt{2} \cdot 288K = 407$ K, a linearization would be not permitted. Therefore, the linearization implicitely assumes the above heat capacity and fast rotation arguments.

In section 4, I now explicitly write Fig. 8 shows the seasonal amplitude for the $C_p$-scenarios as indicated by the blue and dashed black lines, respectively. The larger the seasonal contrast, the colder is the climate. Let us define here $\bar{\cdot}$ as the averaging over a time period (here the seasonal cycle), then $\overline{T^4} > \overline{T}^4$ which is consistent with Hölder's inequality (Rodgers, 1888; Hölder 1889; Hardy et al., 1934, Kuptsov, 2001). It is noted that this feature is missing in the linearized version $A + B \cdot T'$ of the outgoing radiation. We see the large variation in the seasonal cycle $\Delta T = T_{summer} - T_{winter}$ for the blue line in Fig. **??** as compared to the dashed line. A mean change in the net long wave radiation can be approximated by the mean of summer and winter values $\epsilon\sigma \cdot 0.5(T^4_{summer} + T^4_{winter})$, which is up to $10 W m^{-2}$ higher than $\epsilon\sigma \cdot (0.5 \cdot (T_{summer} + T_{winter}))^4$ if the seasonal cycle is damped as in the dashed line of Fig. 8. This implies that a lower seasonal cycle provides for a significant warming. If we would consider a linear model $A + B \cdot T'$ with $T'$ being measured in $°C$ for the long-wave radiation, the differences between the blue and the dashed line would be much lower, due to the absence of the non-linearity in net long wave radiation change.

This clarifies the difference between a linear and non-linear model.